NASA CR-163,744

NASA-CR-163744
19810004432

A Reproduced Copy

OF

NASA CR-163,744

Reproduced for NASA

by the

NASA Scientific and Technical Information Facility

LIBRARY COPY

FEB 15 1989

LANGLEY RESEARCH CENTER
LIBRARY NASA
HAMPTON, VIRGINIA

FFNo 672 Aug 65

NF01723

3 1176 01327 9253

5030-471

Electric & Hybrid Vehicle System
Research & Development Project

(NASA-CR-163744) AERODYNAMIC DESIGN OF ELECTRIC AND HYBRID VEHICLES: A GUIDEBOOK (Jet Propulsion Lab.) 92 p HC A05/MF A01 CSCL 13F

N81-12943

Unclas
G3/85 29312

Aerodynamic Design of Electric and Hybrid Vehicles: A Guidebook

D. W. Kurtz

September 30, 1980

Prepared for
U.S. Department of Energy
Through an agreement with
National Aeronautics and Space Administration
by
Jet Propulsion Laboratory
California Institute of Technology
Pasadena, California

(JPL PUBLICATION 80-69)

DEC 1980
RECEIVED
NASA STI FACILITY
ACCESS DEPT.

N81-12943 #

5030-471

Electric & Hybrid Vehicle System
Research & Development Project

Aerodynamic Design of Electric and Hybrid Vehicles: A Guidebook

D. W. Kurtz

September 30, 1980

Prepared for
U.S. Department of Energy
Through an agreement with
National Aeronautics and Space Administration
by
Jet Propulsion Laboratory
California Institute of Technology
Pasadena, California

(JPL PUBLICATION 80-69)

The research described in this publication was carried out by the Jet Propulsion Laboratory, California Institute of Technology, and was sponsored by the United States Department of Energy through an agreement with NASA.

This report was prepared as an account of work sponsored by the United States Government. Neither the United States nor the United States Department of Energy, nor any of their employees, nor any of their contractors, subcontractors, or their employees, makes any warranty, express or implied, or assumes any legal liability or responsibility for the accuracy, completeness or usefulness of any information, apparatus, product or process disclosed, or represents that its use would not infringe privately owned rights.

This document is available to the U.S. public through the National Technical Information Service, Springfield, Virginia 22161

PREFACE

The Electric and Hybrid Vehicle (EHV) Research, Development and Demonstration Act of 1976, Public Law 94-413, later amended by Public Law 95-238, established the governmental EHV policy and the current Department of Energy EHV Program. The EHV System Research and Development Project, one element of this Program, is being conducted by the Jet Propulsion Laboratory (JPL) of the California Institute of Technology through an agreement with the National Aeronautics and Space Administration. An objective of the Program is to develop the technologies required by the EHV industry to successfully produce vehicles with widespread acceptance. One of those technologies requiring development is vehicle aerodynamics. This guidebook presents the tools, strategies and procedures involved in the design of aerodynamically efficient vehicles. The methodology is intended to be useful to designers possessing little or no aerodynamic training.

ABSTRACT

A typical present-day subcompact EHV, operating on an SAE J227a D driving cycle, consumes up to 35% of its road energy requirement overcoming aerodynamic resistance. The application of an integrated system design approach, where drag reduction is an important design parameter, can increase the cycle range by more than 15%. This guidebook highlights a logic strategy for including aerodynamic drag reduction in the design of electric and hybrid vehicles to the degree appropriate to the mission requirements. Backup information and procedures are included in order to implement the strategy. Elements of the procedure are based on extensive wind tunnel tests involving generic subscale models and full-scale prototype EHVs. The user need not have any previous aerodynamic background. By necessity, the procedure utilizes many generic approximations and assumptions resulting in various levels of uncertainty. Dealing with these uncertainties, however, is a key feature of the strategy.

PRECEDING PAGE BLANK NOT FILMED

CONTENTS

I. INTRODUCTION ---------- 1

II. APPROACH ---------- 5

III. AERODYNAMIC DESIGN LOGIC PATH ---------- 7

A. LEVEL I DESIGN ---------- 8

B. LEVEL II DESIGN ---------- 9

C. LEVEL III DESIGN ---------- 11

D. CONCLUDING REMARKS ---------- 14

IV. REFERENCES ---------- 15

V. BIBLIOGRAPHY ---------- 17

A. GENERAL AUTOMOTIVE AERODYNAMICS ---------- 17

B. FACILITY TESTING ---------- 22

C. ROAD TESTING ---------- 25

D. WIND NOISE ---------- 26

E. VENTILATION AND ENGINE COOLING ---------- 27

F. STABILITY AND HANDLING ---------- 27

G. GENERAL BOOKS AND PROCEEDINGS ---------- 28

APPENDIXES

A. EFFECTS OF ASPECT RATIO AND FINENESS RATIO ON THE AERODYNAMIC CHARACTERISTICS OF AUTOMOBILE SHAPES ---------- 29

B. FOUNDATIONS OF AERODYNAMIC DESIGN ---------- 35

C. A REVIEW OF GENERAL AERODYNAMIC DRAG PREDICTION PROCEDURES, APPLICATION, AND UTILITY ---------- 55

D. APPLICATION OF AREA-DISTRIBUTION SMOOTHING PROCEDURES TO AUTOMOTIVE AERODYNAMIC DESIGN ---------- 69

PRECEDING PAGE BLANK NOT FILMED

E. ESTIMATING DRAG CHARACTERISTICS IN YAW FOR AUTOMOBILE SHAPES ---------- 77

F. DETERMINATION OF DRAG WIND WEIGHTING FACTORS FOR VEHICLES OPERATING IN AMBIENT WINDS ---------- 81

Figures

1-1. Road Energy Component Split Over the SAE J227a Schedule D Driving Cycle ---------- 2

1-2. Projected Vehicle Range Over the SAE J227a Schedule D Driving Cycle as a Function of Various Parameters ---------- 2

3-1. Aerodynamic Design Logic Path, Level I ---------- 7

3-2. Aerodynamic Design Logic Path, Level II ---------- 9

3-3. Aerodynamic Design Logic Path, Level III ---------- 12

SECTION I

INTRODUCTION

As an automobile moves along a road surface, the resulting displacement of air gives rise to various forces and moments. Depending upon the mission, or driving cycle, the aerodynamic drag experienced by a typical electric or hybrid vehicle (EHV) may consume a significant portion of the energy supplied by the propulsion system. Since the SAE J227a D cycle has been suggested as being representative of an electric passenger vehicle mission, it is proper to consider the impact of aerodynamic design upon the total road energy requirement for that cycle. Figure 1-1 shows the cycle energy split as a function of drag area, C_DA[1], for a typical subcompact EHV weighing 1350 kg (3000 lb) and having a rolling resistance coefficient of 1.2% of the vehicle weight (rolling losses include those due to tires, bearings, gears, brakes, etc.). Current subcompact-class vehicles have drag areas of about 0.9 m^2 (9.7 ft^2) which means that the aerodynamic component may be responsible for about 35% of the total road energy consumed over this cycle. Because of progress recently demonstrated by the automotive industry, it is reasonable to expect that, with vigorous design efforts, a drag area of 0.55 m^2 (5.9 ft^2) may be achievable. The benefit of such a 40% reduction in the C_DA related to an electric vehicle (EV) is shown, in Figure 1-2, to be nearly a 20% improvement in range. To achieve a similar benefit via reductions in the other components would require about a 50% reduction in the rolling resistance coefficient to 0.6% (a rather unrealistic value) or a 22% reduction in vehicle weight (the removal of an additional 300 kg from an already lightweight vehicle would be very difficult). These examples, although simplified, tend to demonstrate the potential benefits from, and justification for pursuing aerodynamic resistance reduction.

Efficient aerodynamic design is an elusive accomplishment. Automotive aerodynamics is presently at the stage aircraft aerodynamics was 50 years ago. It is, however, a fundamentally different problem since a road vehicle is a bluff body, having many local areas of flow separation, and operates in the presence of the ground. Recognizing the need and potential benefits to be derived from a clearer understanding, the SAE recently commissioned the development of an automotive aerodynamic research plan (Reference 1-1).

---

[1] The drag coefficient, C_D, is nondimensional and is defined as

$$C_D = \text{Drag Force}/(1/2 \times \text{Air Density} \times \text{Velocity}^2 \times \text{Frontal area}).$$

The frontal area, A, is the vehicle's projected area including tires, and suspension members but excluding appendages such as mirrors, roof racks, antennas, etc. The velocity is the relative speed between the air and the vehicle.

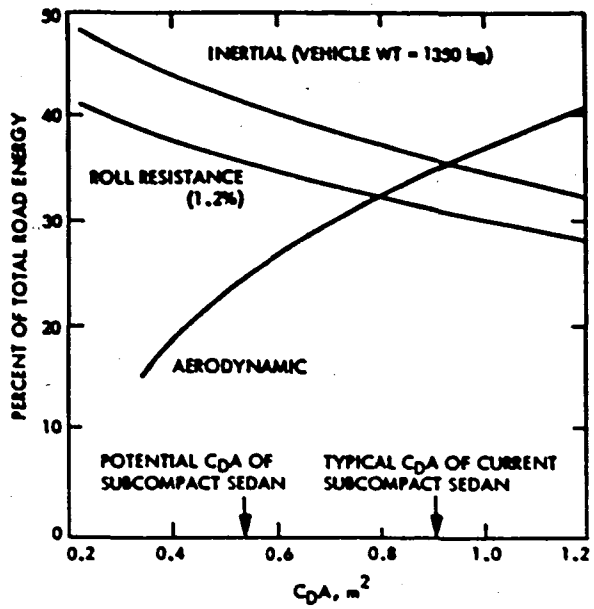

Figure 1-1. Road Energy Component Split Over the SAE J227a Schedule D Driving Cycle

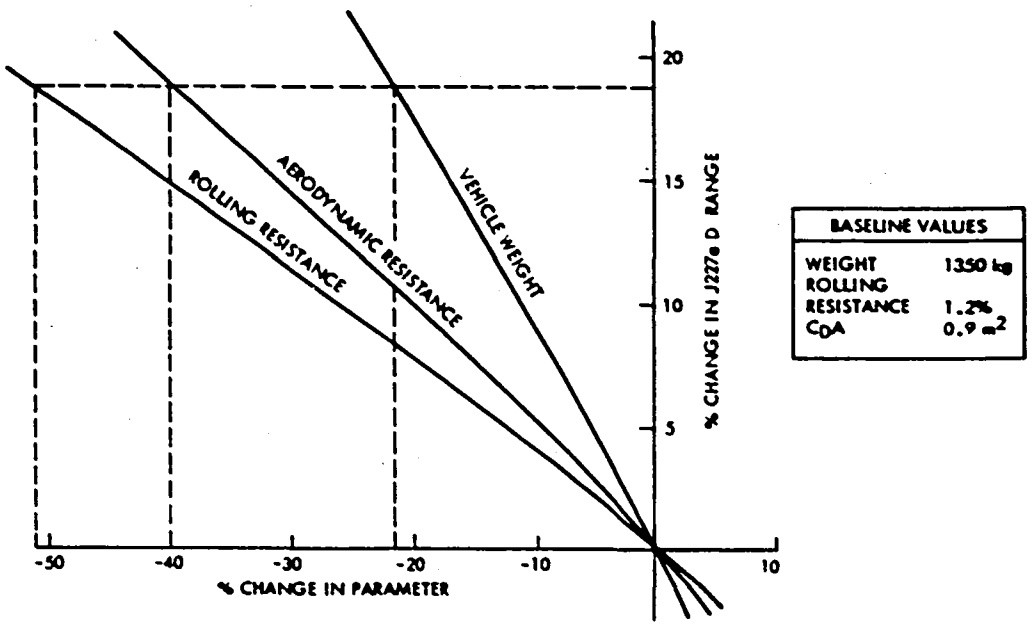

Figure 1-2. Projected Vehicle Range Over the SAE J227a Schedule D Driving Cycle as a Function of Various Parameters

This plan calls for the expenditure of 25 million dollars over a five year period in order to bring the state-of-the-art of automotive aerodynamics into line with other engineering disciplines. The sheer size and commitment indicated by such an undertaking gives one some perspective into the difficulties and uncertainties inherent in automotive aerodynamic design today.

This aerodynamic design guidebook utilizes a logic strategy for designing aerodynamically-appropriate electric and hybrid vehicles with current aerodynamic understanding. Its intended user is the vehicle designer and builder who has little or no aerodynamic background. By necessity, the procedure utilizes many generic approximations and assumptions resulting in various levels of uncertainty. Dealing with these uncertainties, however, is a key feature of the strategy.

SECTION II

APPROACH

The approach is to develop an aerodynamic design sequence composed of logical path elements which provide a strategy and guide through progressively more refined levels of design. The process of developing this logic path exposed many technological gaps and information voids inherent in various path elements. In the course of this endeavor, studies and test programs were undertaken in order to alleviate the uncertainties and to provide the necessary tools and procedures required to implement the strategy.

A limited aerodynamic data base was developed by wind tunnel testing 20 electric, hybrid and subcompact vehicles (Reference 2-1). These results were used to extend, develop and refine drag prediction techniques; to develop generalized relationships between drag and yaw angle (the angle between the relative wind and the longitudinal axis of the car); and to quantify the uncertainty in subscale-to-full-scale wind tunnel test correlations.

Because of battery packaging requirements, EHVs may be subject to somewhat different constraints than conventional internal combustion (IC) engine vehicles. For instance, owing to the use of a central battery tunnel, a small vehicle may be unusually wide or long. A series of subscale tests was therefore performed to determine if aspect ratio and fineness ratio[1] were important aerodynamic parameters.

Since any road vehicle rarely operates in a zero-wind environment, an analysis of the driving cycle-dependent effects of ambient winds on vehicle drag was performed. This is a necessary extension to aerodynamic drag evaluations and should be included in vehicle computer and dynamometer simulations.

Finally, it was necessary to evaluate simplified general aerodynamic design principles in order to determine the confidence levels resulting from their application.

---

[1]Aspect ratio (AR) is defined as body height divided by width, and fineness ratio (FR) as length divided by effective diameter (of equivalent area circle).

SECTION III

AERODYNAMIC DESIGN LOGIC PATH

The logic sequence incorporates path elements which terminate at one of three levels of design. These design levels are progressively more refined and are successively characterized by a higher probability of yielding a low drag design. This logic path, then, defines the procedural elements required for the design of an aerodynamically efficient EHV. Technical backup information is supplied in the various appendixes in order to facilitate applying the procedures.

The strategy which governs the use of these procedures originates in the development of a design acceptability criterion. Consider the design logic path beginning in Figure 3-1. Note that the initial steps are the definition of the mission use or cycle requirements, and the resulting determination of the aerodynamic acceptability criterion. This is the heart, the driver, of the entire process. It is imperative that one carefully characterize the mission performance objectives for which the vehicle is being designed at the outset. Once this is established, a thorough trade-off analysis must be made in order to determine the relative sensitivities of the various physical parameters. The result of such a procedure is analogous to that presented in Figure 1-2. There, the mission performance objective was to maximize range over the SAE J227a Schedule D driving cycle and the resulting sensitivity analysis was

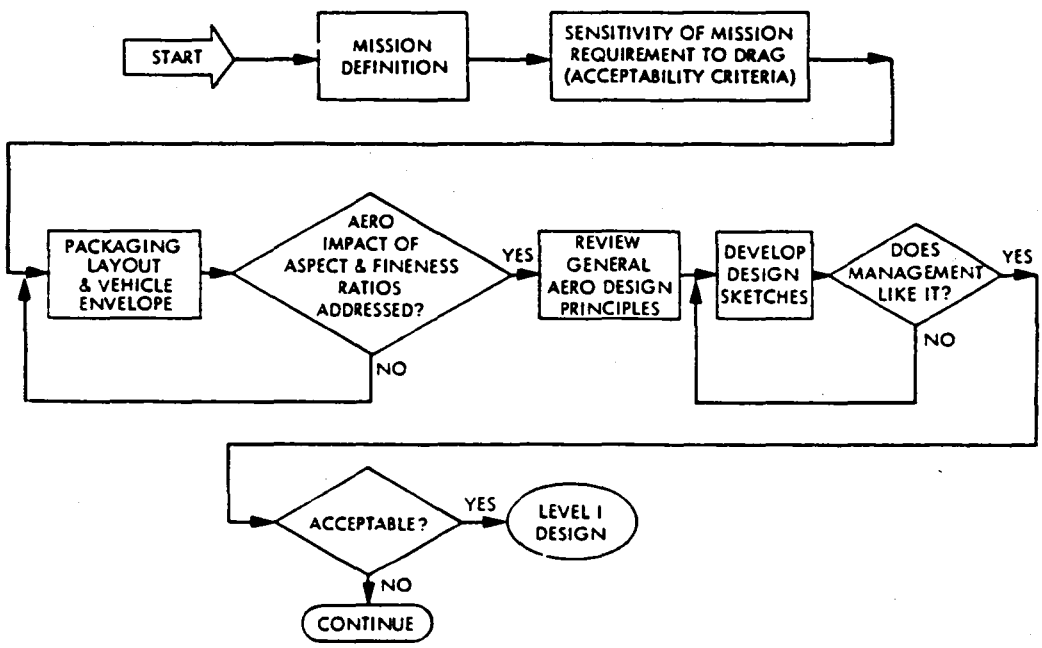

Figure 3-1. Aerodynamic Design Logic Path, Level I

PAGE 6 INTENTIONALLY BLANK

performed (using a simple vehicle computer simulation) around a postulated baseline vehicle[1]. It should be emphasized that these sensitivity relationships are a strong function of the mission requirements.

For instance, if one were designing a postal vehicle or milk delivery truck whose mission is characterized by numerous starts and stops and virtually no constant or high speed cruising, the energy efficiency (or range) would be almost independent of the aerodynamic drag. On the other hand, if a high-speed commuter vehicle characterized by relatively few stops is being designed, the range is a very strong function of the aerodynamic drag. After these parametric sensitivities have been determined for the design mission, a target value and tolerance limit for the vehicle's aerodynamic drag may be established. This becomes the "acceptability criterion" against which various designs will be evaluated throughout the remainder of the procedure.

A. LEVEL I DESIGN

The first level of design (Figure 3-1) focuses primarily on the gross and superficial design processes characteristic of a designer's sketchbook. This may be called a subjective design analysis and is an essential beginning to any design process. First, the packaging layout and vehicle envelope must be determined. For IC engine vehicle design, this is influenced primarily by the passengers, payload and drivetrain volume requirements. For electric vehicles, the significant additional volume required for the traction batteries could impact the normal body proportions to such a degree that any first order aerodynamic influence needs to be addressed. That is, with the use of a central battery tunnel, a small car may be unusually wide; or with batteries located beneath seats (or under the floorboard), the vehicle may be unusually tall. The aerodynamic consequence is such that the specific effects of aspect ratio and fineness ratio can be identified and should be considered. Subscale tests were conducted on a family of automotive shapes in order to quantify their influence on drag. The generic trends and relationships appear in Appendix A. After iterating this trade-off within the bounds of the design theme and utility requirements, the next path element may be addressed. This is characterized as a general review and understanding of the sources of automotive drag and some of the basic principles involved in efficient aerodynamic design. A brief treatise on the subject appears in Appendix B.

With the packaging envelope and general aerodynamic guidelines in hand, the first body design sketches can begin to evolve. As a styling theme is developed and refined, the final sketches are reviewed and, after several iterations, proposed design drawings are

---

[1]The sensitivity analysis can be done for other performance objectives as well (e.g., acceleration, gradeability, etc.).

selected. The aerodynamic acceptability criterion, determined in the first steps, is now applied. Note that no quantitative aerodynamic analysis has been performed to this point; therefore, there is considerable uncertainty as to the value of the drag coefficient represented by this design. The probability of it being an exceptionally low-drag design is quite small. If, however, the sensitivity analysis performed earlier indicated a weak dependence of the performance objective (e.g., range) on the drag level, the large uncertainty may be perfectly acceptable. That is, there would be no justification for refining the aerodynamic design any further, and the Level I design would yield a vehicle having "appropriate aerodynamic design" commensurate to its mission. If, on the other hand, the sensitivity analysis had indicated a stronger dependence on drag level and the resulting acceptability criterion had required that the drag coefficient be no greater than, say 0.5, then Level I Design, with its characteristically large uncertainty, would be unacceptable. If such were the case, continuation to the next level of design would then be required.

B. LEVEL II DESIGN

The second level of design (Figure 3-2) can be described as an empirical design analysis utilizing procedures and practices which are generically effective. The final sketches resulting from the Level I design procedures become a baseline or strawman design for the Level II analysis.

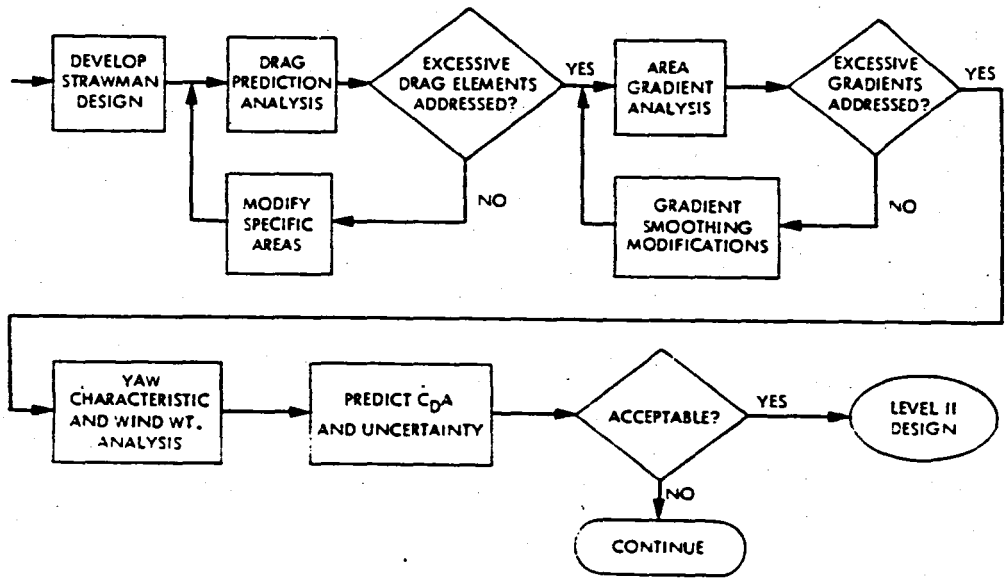

Figure 3-2. Aerodynamic Design Logic Path, Level II

Drag prediction for automotive shapes is generally unreliable in an absolute sense; its real value lies in the possibility of highlighting various drag producing elements. These drag prediction procedures (Appendix C) are a drag buildup approach (References 3-1, 3-2, and 3-3). That is, the vehicle is divided up into about a dozen regions and the drag contribution from each region is then determined by examining the local shape characteristics. By noting the relative magnitude of various drag elements, those regions deserving of more attention are identified. Any necessary modifications can be factored in and reevaluated in an iterative manner.

A general principle associated with low-drag vehicle design is the desirability of maintaining attached flow. Regions of separated flow give rise to pressure drag increments. Even if it remains locally attached, each time the flow bends in order to follow a body contour, it gives up a portion of its kinetic energy. Because of the resulting momentum loss, the successful negotiation of subsequent contours becomes less probable and the onset of separation at some other marginal point on the vehicle is more likely to occur. For these reasons, it has been postulated (References 3-4 and 3-5) that the drag produced by a vehicle moving through a fluid may be reduced by minimizing the body contour gradients. A possible corollary to that premise is that the rate of change of vehicle cross-sectional area with longitudinal station is representative of the integral of all the local body contours. Adopting that premise, the "area distribution" procedure (Appendix D) is applied to the strawman design yielding a plot of cross-sectional area versus longitudinal station at about 10-cm intervals. Those regions where the area is rapidly changing are candidates for subtle modification. Certain unavoidable lumps and bumps occur in the neighborhood of the tires and wheelhouses, but some smoothing may be possible in the transition regions.

Since a vehicle rarely operates in a zero-wind environment, the instantaneous drag coefficient is a function of the local relative yaw angle. Therefore, knowledge of the drag versus yaw characteristic is required. A general equation describing this relationship as a function of generic vehicle shape parameters (developed from References 2-1 and 3-6) is presented in Appendix E. The effective drag experienced by a vehicle can be evaluated by figuratively driving the vehicle over a prescribed velocity-time schedule in the presence of a time-variant wind which is statistically probable from any direction (Reference 3-7). The resultant combination of the vehicle velocity and wind vector distribution yields an instantaneous yaw angle with respect to the vehicle. With the vehicle's drag-yaw characteristic known, the resultant drag may be determined at each instant. Therefore, the energy required to overcome aerodynamic resistance can be calculated by integrating the instantaneous aerodynamic power required over the cycle. It is then possible to determine what constant drag coefficient would have been necessary in order to yield the same result. The ratio of this new effective coefficient, $C_{D_{eff}}$, to the original zero-yaw drag coefficient

(C_{D_o}) is the wind weighting factor, F. A simplified procedure for calculating F is presented in Appendix F.

Relative to the result of Level I Design, the uncertainty band associated with this Level II effective drag coefficient prediction is considerably narrowed. One should expect that, at the conclusion of the Level II analysis, the drag prediction uncertainty band will be of the order of ±15%. That result is again evaluated according to the previously-developed acceptability criterion. If the design requirements are satisfactorily met, then the Level II Design represents an "appropriate aerodynamic design" and the process is complete. If either a lower drag value or less uncertainty is demanded by the acceptability criterion, Level II design is inadequate, and one must continue on to a further level of design refinement.

C. LEVEL III DESIGN

The third and most-refined level of design is an experimental process relying heavily on insight and experience. Persons having some knowledge of experimental automotive aerodynamic techniques should be involved (e.g., a consultant) or little can be gained by this process. In addition, a relatively large financial commitment must be undertaken in order to proceed. Up to this point, no procurements have been required, no hardware has been created and the total effort expended has been a few man-months. Building models and performing developmental wind tunnel tests may increase these aerodynamic design related costs by a factor of 10 or more. If that level of expenditure is warranted, Level III Design should be initiated (Figure 3-3).

Utilizing the results of the Level II design process, a subscale wind tunnel model is constructed. Since the objective of these tests is to fine tune the design, a model with the capability of incorporating subtle changes is required. A special clay surface laid on a rigid substructure has proved to be the most practical approach. The model scale and support details are functions of the specific wind tunnel being used. Quarter to three-eighths scale have been the most popular.[1] It is highly recommended that the level of model detail and scale fidelity be guided by an automotive aerodynamicist and the construction be performed by professional model builders with specific wind tunnel experience. Improperly-constructed models can yield misleading results, or even worse, disintegrate due to the airloads experienced in a wind tunnel.

---

[1] In order to minimize controversial wind tunnel wall corrections, the model scale should be chosen such that the model cross-sectional area be no more than 6% of the tunnel cross-sectional area (above the ground plane).

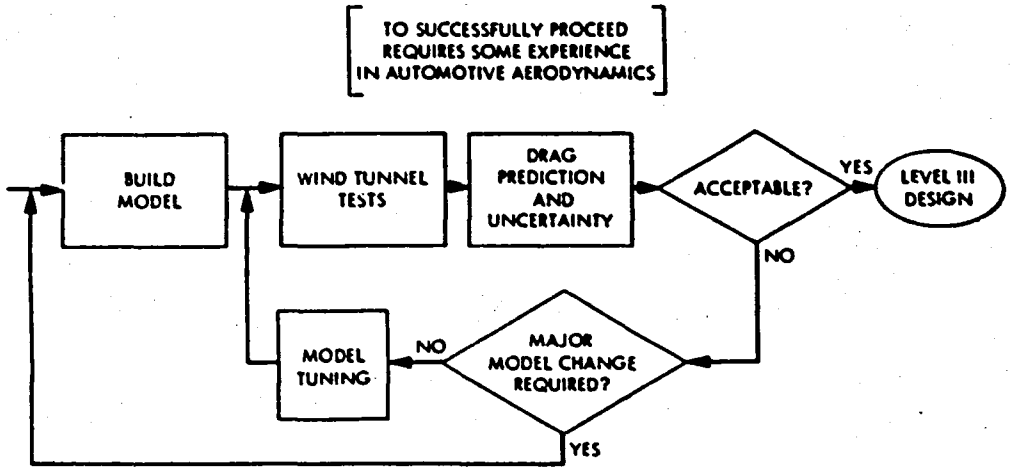

Figure 3-3. Aerodynamic Design Logic Path, Level III

A minimum of 15 to 20 wind tunnel occupancy hours will be required for testing of the preliminary model in original and slightly-modified forms (sometimes called, "aerodynamic tuning"). This is in addition to initial shakedown runs to check out the model construction, verify that the data acquisition and tunnel systems are operating properly and to quantify the effects of Reynolds Number (sensitivity of aerodynamic coefficients to air speed). Usually, the effect is small and a convenient tunnel air speed[1] can be adopted for the rest of the test. If a real-time data reduction system is provided, the model drag coefficient can be continuously monitored. Tests should be performed at yaw angles up to about 40 degrees in order to develop the information necessary for the wind weighting analysis (Appendix F). Applying factors to account for subscale to full-scale correlations,[2] a drag prediction and associated uncertainty may be determined. The acceptability criterion is applied as described earlier.

If the criterion were immediately satisfied at this point, the design process could be concluded. However, the expense and effort committed to model testing plus the ever present uncertainty band (due largely to unavoidable body panel surface misalignments in the

---

[1] The speed should be high enough to get good resolution on the loads being measured (a function of the balance system).

[2] This is a function of the model level of detail and the particular subscale wind tunnel and data reduction procedures. Calibration models are currently being tested in all the major subscale and full-scale tunnels in the country (and abroad).

production vehicle) warrants some further testing.[1] For instance, since stabilized flow attachment is an attribute of low drag designs, a means of observing local surface flow behavior is desirable.

- Several methods exist and each has advantages and disadvantages. Attaching rows of soft, flexible yarn tufts is simple, inexpensive, easy to photograph and effectively highlights flow instabilities; it does, however, modify the surface detail by its very presence and can consequently affect the absolute level of the data. An alternative is the use of ink drops (or other visible fluids) which, when placed on the surface spread out and indicate the path of the streamlines on the vehicle surface with very little flow interference; the disadvantages of the technique are its transient nature, gravity effects as the droplet spreads along the body side and the mess.
  Seeding the airflow with smoke or particulates is another approach. This usually has many tunnel operational considerations which may prove unsatisfactory. Often, the ink drop approach is preferred on clay models since tuft attachment may be difficult. Flow separation and instabilities are easily identified. With a combination of engineering judgment and artistic style, the clay surface is iteratively altered in order to develop a smooth, stable flow pattern. It is extremely important to document each alteration with pictures, measurements and templates, as it is often necessary to return to an intermediate configuration before continued progress can be made. Front underbody air dams (chin spoilers) and rear deck spoilers (lips) can often provide beneficial results if properly designed and located (References 3-8 and 3-9). A good candidate device should be effective through a reasonable range of yaw angles. Drag data should be continuously monitored in order to help guide the process. If, after repeated attempts, large areas of flow separation still exist, major model contour or shape modifications may be necessary. If the flow is everywhere stabilized and the rear separation point is such that the wake size is minimized, further significant drag reduction is unlikely. Pressure taps may be installed in the surface of the model in order to optimally locate the inlets and exits for interior ventilation. If high-mass flow ram air is required for motor or engine (hybrid) cooling, it would be wise to construct a model with properly scaled internal flow path ducts. Not only is there a drag component associated with the internal flow losses, but the condition may significantly alter the flow over the outer surface of the vehicle as well.

Little more can be accomplished in model scale. Owing to local Reynolds number, scale fidelity and flow conditions, the absolute drag levels measured in test are rarely substantiated in full-scale tests on the prototype or production vehicle; full-scale test results are often 10 to 20% greater (Reference 3-10), thus contributing to a rather large uncertainty even at this point. Experience and correlations from previous subscale and full-scale tests in the same

---

[1]Because model installation and setup is not a trivial matter, tunnel test time is usually contracted for a 6-8 hr minimum.

facilities can reduce the uncertainty to about ±5%. As an ultimate step, aerodynamic tuning on a full-scale replica may be considered. The expense involved in building a single-purpose wind tunnel model may not be warranted; however, a full-scale mock-up or male buck might be suitably altered for test purposes. To make that step worthwhile, special attention should be paid to the underbody and internal flow details.

D. CONCLUDING REMARKS

This process should not be considered to be a mindless formula for success. Rather, it is a framework upon which the design development is built. The procedures are highly dependent upon many subjective determinations which rely heavily upon common sense and experience. There may be many alternative solutions to the same set of design requirements.

The objective behind the creation of the design guide is to encourage EHV designers to address aerodynamic drag as an important design parameter[1]; and once goals are targeted, to systematically evolve a design which is aerodynamically matched to the anticipated mission while minimizing unnecessary effort.

---

[1]Unlike high-speed sports and competition vehicles which rely heavily on aerodynamic forces for such things as traction and stability, the conventional road vehicle is primarily concerned with the drag component. This is not the say that the other five aerodynamic components are not of interest, but unless unusual operational conditions are anticipated, low drag optimization is usually pursued without compromise.

SECTION IV

REFERENCES

1-1. Milliken, W. F., Aerodynamic Research Plan for Automotive-Type Vehicles, prepared for the Society of Automotive Engineers, Inc., Oct. 1977.

2-1. Kurtz, Donald W., Aerodynamic Characteristics of Sixteen Electric, Hybrid, and Subcompact Vehicles - Complete Data, JPL Publication 79-59, June 1978.

3-1. White, R. G. S., A Method of Estimating Automobile Drag Coefficients, SAE Paper No. 690189, Detroit, MI, Jan. 1979.

3-2. Pershing, B., and Masaki, M., Estimation of Vehicle Aerodynamic Drag, EPA-46013-76-025 Aerospace Corporation, 1976.

3-3. Smalley, W. M., and Lee, W. B., Assessment of an Empirical Technique for Estimating Vehicle Aerodynamic Drag from Vehicle Shape Parameters, ATR-78 (7623-03)-1, Aerospace Corporation, July 1978.

3-4. Hucho, W. H., "The Aerodynamic Drag of Cars - Current Understanding, Unresolved Problems and Future Prospects", Aerodynamic Drag Mechanisms of Bluff Bodies and Road Vehicles, General Motors Symposium, Detroit, MI, Sept. 1976.

3-5. Morelli, A., Fioravanti, L., and Cogotti, A., The Body Shape of Minimum Drag, SAE Paper No. 760186, Detroit, Feb. 1976.

3-6. Bowman, William D., Generalizations on the Aerodynamic Characteristics of Sedan Type Automobile Bodies, SAE Paper No. 660389, Detroit, Jan. 1966.

3-7. Dayman, Bain, Jr., Realistic Effects of Winds on the Aerodynamic Resistance of Automobiles, SAE Paper No. 780337, Detroit, Feb. 1978.

3-8. Marte, J. E., Weaver, R. W., Kurtz, D. W., and Dayman, B., A Study of Automobile Aerodynamic Drag, DOT-TSC-OST-75-28, Sept. 1975.

3-9. Schenkel, F. K., The Origins of Drag and Lift Reductions on Automobiles with Front and Rear Spoilers, SAE Paper No. 770389, Feb. 1977.

3-10. Kurtz, Donald W., The Development of a Low-Drag Body Shape for the ETV-1 Electric Vehicle, JPL 5030-438, Dec. 1979.

B-1. Klemperer, W., "Luftwiderstandsuntersuchungen an Automobilmodellen," Zeitschrift F. Flugtechnik und Motorluftschiffahrt 13 (1922), S. 201-206.

B-2. Autoweek, May 26, 1978.

B-3. Korff, W.H., The Aerodynamic Design of the Goldenrod--to Increase Stability, Traction and Speed, SAE Paper No. 660390.

B-4. Kelly, K.B., and Holcombe, H.J., Aerodynamics for Body Engineers, SAE Paper No. 649A, Jan. 1963.

B-5. Paish, M.G., and Stapleford, W.R., A Study to Improve the Aerodynamics of Vehicle Cooling Systems, MIRA Report 1968/4, Dec. 1967.

B-6. Emmenthal, K.D., and Hucho, W.H., A Rational Approach to Automotive Radiator Systems Design, SAE Paper No. 740088, Feb. 1974.

B-7. Olsen, M.E., Aerodynamic Effects of Front End Design on Automobile Engine Cooling System, SAE Paper No. 670188, Feb. 1976.

C-1. Cornish, J.J., and Fortson, C.B., Aerodynamic Drag Characteristics of Forty-Eight Automobiles, Miss. St. Aerophysics Dept. Res. Note No. 23, June 1964.

C-2. Fluid Dynamic Drag, Hoerner, Sighard F., published by the author, 1958.

C-3. Ohtani, K., et al., Nissan Full-Scale Wind Tunnel--Its Application to Passenger Car Design, SAE Paper No. 720100, Detroit, MI, 1972.

C-4. Carr, G.W., Reducing Fuel Consumption by Means of Aerodynamic "Add-on" Devices, SAE Paper No. 760187, Detroit, MI, 1976.

C-5. Korff, W.H., The Body Engineer's Role in Automotive Aerodynamics, SAE Paper No. 649B, Automotive Engineering Congress, Jan. 1963.

D-1. "Body Shaping You Don't See", Design News, May 5, 1980.

E-1. Barth, R., "Effect of Unsymmetrical Wind Incidence on Aerodynamic Forces Acting on Vehicle Models and Similar Bodies" (report abstracted from 1958 Stuttgart thesis), A.T.Z., Mar. and Apr. 1960, pp. 89-95, MIRA Translation 15/60.

SECTION V

BIBLIOGRAPHY

Over 160 reports, papers and books on various aspects of automotive aerodynamic design are organized into the following categories:

- General Automotive Aerodynamics
- Facility Testing
- Road Testing
- Wind Noise
- Ventilation and Engine Cooling
- Stability and Handling
- General Books and Proceedings

A. GENERAL AUTOMOTIVE AERODYNAMICS

Barth, R., "Effect of Unsymmetrical Wind Incidence on Aerodynamic Forces Acting on Vehicle Models and Similar Bodies" (report abstracted from 1958 Stuttgart thesis), A.T.Z., Mar. and Apr. 1960, pp. 89-95, MIRA Translation 15/60.

Barth, R., "Effect of Shape and Airflow about an Automobile on Drag, Lift, and Direction Control," VID, Vol. 98, No. 22, p. 1265 (in German), Aug. 1, 1956.

Bettes, W.H., "Aerodynamic Testing of High-Performance Land-Borne Vehicles - A Critical Review" in AIAA Symposium on the Aerodynamics of Sports and Competition Automobiles, Los Angeles, CA, Apr. 1968.

Bez, U., Messung des Luftwinderstandes von Kraftfahrzeugen durch Auslaufversuche, Research report, Dipl. Engr. Thesis, Tech. Univ. at Stuttgart, and Porsche Research Rept., Jan. 1972.

Bowman, W.D., "The Present Status of Automobile Aerodynamics in Automobile Engineering & Development," AIAA Symposium on the Aerodynamics of Sports and Competition Automobiles, Los Angeles, CA, Apr. 1968.

Bowman, W.D., "Generalizations on the Aerodynamic Characteristics of Sedan-Type Automobile Bodies," SAE Preprint 660389, June 6-10, 1966, SAE Transactions, June 1967.

Boyce, T.R., and Lobb, P.J. (U.K.), "An Investigation of the Aerodynamics of Current Group 6 Sport Car Designs," 'Advances in Road Vehicle Aerodynamics' 1973, pp. 127-145, BHRA Fluid Engineering, 1973.

Buckley, B. Shaw, Laitone, Edmund V., Airflow Beneath an Automobile, SAE Paper No. 741028, Oct. 1974.

Burst, H.E., and Srock, Lainer, The Porsche 924 Body - Main Development Objectives, SAE Paper No. 770311, Detroit, MI, 1977.

Carr, G.W., The Aerodynamics of Basic Shapes for Road Vehicles, Part 2: Saloon Car Bodies, MIRA Rept. No. 1968/69.

Carr, G.W., The Aerodynamics of Basic Shapes for Road Vehicles, Part 1: Simple Rectangular Bodies, MIRA Rept. No. 1968/2.

Carr, G.W., Correlation of Aerodynamic Force Measurements in Quarter-and Full-Scale Wind Tunnels (Second Report), MIRA Rept. 1967/1.

Carr, G.W., The Development of a Low Drag Body Shape for a Small Saloon Car, MIRA Bulletin No. 2, pp. 8-14, 1965.

Carr, G.W., Aerodynamic Effects of Modifications to a Typical Car Model, MIRA Rept. No. 1963/4.

Carr, G.W., Aerodynamic Effects of Underbody Details on a Typical Car Model, MIRA Report 1965/7.

Carr, G.W., Reducing Fuel Consumption by Means of Aerodynamic 'Add-on Devices', SAE Paper No. 760187, Feb. 1976.

Choulet, R., Favero, J.L., and Romani, L., "A Study of the Aerodynamic Interaction Between a Lorry and a Car," Advances in Road Vehicle Aerodynamics 1973, pp. 255-270, BHRA Fluid Engineering, 1973.

Cornish, J.J. III, "Some Aerodynamic Characteristics of Land Vehicles," in AIAA Symposium on the Aerodynamics of Sports and Competition Automobiles, Los Angeles, CA, Apr. 1968.

Cornish, J.J., Some Considerations of Automobile Lift and Drag, SAE Paper 948B, Jan. 11-15, 1965.

Cornish, J.J., and Fortson, C.B., Aerodynamic Drag Characteristics of Forty-Eight Automobiles, Miss. St. Aerophysics Dept. Res. Note No. 23, June 1964.

Crackrell, J.E., and Harvey, J.K. (Imp. Col., U.K.), "The Flow Field and Pressure Distribution of an Isolated Road Wheel", 'Advances in Road Vehicle Aerodynamics' 1973, pp. 155-168, BHRA Fluid Engineering, 1973.

Flynn, H., and Kyropoulos, P., Truck Aerodynamics, SAE Preprint 284A, 1961.

Fogg, A., and Brown, J.S., Some Experiments on Scale-Model Vehicles with Particular Reference to Dust Entry, MIRA Report No. 1948/1.

Fosberry, R.A.C., The Aerodynamics of Road Vehicles - A Survey of the Published Literature, MIRA Report 1958/1, p. 25.

Fugerson, W.T., "Aerodynamic Drag," Road and Track, pp. 92-98, Mar. 1966.

Grotewohl, A., "Seitenwinduntersuchungen an Personenwagen ("Investigating the Effects of Cross Winds on Passenger Vehicles") Part I, A.T.Z., Vol. 69, No. 11, pp. 377-381, MIRA Translation No. 3/68, Nov. 1967.

Hawks, R.J., and Sayre (U. of Md.), "Aerodynamics and Automobile Performance," 'Advances in Road Vehicle Aerodynamics' 1973, pp. 1-13, BHRA Fluid Engineering, 1973.

Hawks, R.J., A Tentative Model for Automobile Aerodynamics, MIT, 1966.

Hoerner, S.F., "Fluid-Dynamic Drag," published by author (148 Busteed Dr., Midland Park, NY), 1965.

Hogue, J.R., Aerodynamics of Six Passenger Vehicles Obtained from Full Scale Wind Tunnel Tests, SAE Paper No. 800142, Detroit, MI, 1980.

Howell, J.P. (City Univ., U.K.), The Influence of the Proximity of a Large Vehicle on the Aerodynamic Characteristics of a Typical Car," 'Advances in Road Vehicle Aerodynamics' 1973, pp. 207-221, BHRA Fluid Engineering, 1973.

Hucho, W.H., Jansen, L.J., and Schwartz, G., The Wind Tunnel's Ground Plane Boundary Layer - Its Interference with the Flow Underneath Cars, SAE Paper No. 750066, Feb. 1975.

Hucho, W.H., Jansen, L.J., and Emmelmann, H.H., The Optimization of Body Details - A Method of Reducing the Aerodynamic Drag of Road Vehicles, SAE Paper No. 760185, Feb. 1976.

Jansen, L.J., and Hucho, W.H. (Volkswagenwerk AG, Ger. Fed. Republic), "The Effect of Various Parameters on the Aerodynamic Drag of Passenger Cars," 'Advances in Vehicle Aerodynamics' 1973, pp. 223-254, BHRA Fluid Engineering. 1973.

Jansen, L.J., and Emmelmann, H.H., Aerodynamic Improvements - A Great Potential for Better Fuel Economy, SAE Paper No. 780265, Feb. 1978.

Kelly, K.B., Kyropoulos, P., and Tanner, W.F., Automobile Aerodynamics, SAE Preprint No. 148B, SAE National Automobile Meeting, Detroit, MI, Mar. 1969.

Kirsch, J.W., Garth, S.H., and Bettes, W., Drag Reduction of Bluff Vehicles with Airvanes, SAE Paper No. 730686, 1973.

Klemperer, W., "Investigations of the Aerodynamics of Automobiles," Zeitschrift fuer Flugtechnik, Vol. 13, p. 201 (in German), 1922.

Koenig-Fachsenfeld, R., "Aerodynamics of Motor Vehicles," Motor Rundschau Verlag, Frankfurt A.M. (in German), 1951.

Korff, W.H., The Body Engineer's Role in Automotive Aerodynamics, SAE Paper No. 649B, Jan. 1963.

Kosier, T.D., and McConnell, W.A., "What the Customer Gets" SAE Symposium: Where Does All the Power Go?, SAE No. 783, June 1956.

Kuchemann, D., and Weber, J., "Aerodynamics of Propulsion," McGraw-Hill Publications in Aeronautical Science.

Kurtz, D.W., Aerodynamic Resistance Reduction of Electric and Hybrid Vehicles - A Progress Report, September 1978, HCP/M5030-274 (NTIS), Apr. 1979.

Kurtz, D.W., Aerodynamic Characteristics of Sixteen Electric, Hybrid and Subcompact Vehicles - Complete Data, DOE/JPL/152170, June 1979.

Kurtz, D.W., The Development of a Low-Drag Body Shape for the ETV-1 Electric Vehicle - Results from 3/8 Scale and Prototype Wind Tunnel Tests, JPL 5030-438, Dec. 1979.

Kurtz, D.W., A Systems Approach to EHV Aerodynamic Design, Conference Proceedings, EV Expo '80, Electric Vehicle Council, St. Louis, MO. May 1980.

Kyropoulos, P., Kelly, K.B., and Tanner, W.F., Automotive Aerodynamics, SAE Paper No. Sp-180, Mar. 1960.

Lamar, P., "Aerodynamics and the Group Seven Racing Car," in AIAA Symposium on the Aerodynamics of Sports and Competition Automobiles, Los Angeles, CA, Apr. 1968.

Larrabee, E.E., Road Vehicle Aerodynamics or Aerodynamics as an Annoyance, seminar paper presented at the Cranfield Institute of Technology, June 1973.

Lay, W.E., "Is 50 Miles per Gallon Possible with Correct Streamlining?," SAE Journal, Vol. 32, p. 144, 1933.

Lind, Walter, G.I., "Car Aerodynamics," Automobile Engineer, June 1958.

Lobb, P.J., The Aerodynamic Effects on Group VI Racing Cars, M.Sc. thesis, Imperial College of Science, London University, 1971.

Mair, W.A., "Reduction of Base-Drag by Boat-Tailed Afterbodies in Low-Speed Flow," Aeronautical Quarterly, Nov. 1969.

Marcell, R.P., and Romberg, G.F., "The Aerodynamic Development of the Charger Daytona for Stock Car Competition," Paper 70036, SAE Automotive Engr. Congress, Detroit, MI, Jan. 1970.

Marte, J.E., et al., A Study of Automobile Aerodynamic Drag, DOT-TSC-OST-75-28, Sept. 1975.

Matthews, S.A., Aerodynamic Studies Affecting Car Performance and Appearance, Ford Motor Co. of England, Apr. 1962.

McLean, R.F., and Schilling, R., "Behind the Firebird Car's New Look," SAE Journal, Vol. 62, p. 40, Aug. 1954.

Milliken, William, and Zlotnick, Martin, Aerodynamics of Road Vehicles, AIAA Paper No. 79-0531, Washington, DC, Feb. 1979.

Moller, E., "Drag Measurements on the VW Delivery Truck, "ATZ, Vol. 53, No. 6, p. 153, June 1951.

Morel, T., Aerodynamic Drag of Bluff Body Shapes Characteristic of Hatch-Back Cars, SAE Paper No. 780267, Feb. 1978.

Morelli, A., "Aerodynamic Action on an Automobile Wheel," Symposium on Road Vehicle Aerodynamics, Paper No. 5, The City University, 1969.

Morelli, A., "Theoretical Method for Determining the Lift Distribution on a Vehicle," F.I.S.I.T.A., 1964.

Morelli, A., Fioravanti, L., and Cogotti, A., The Body Shape of Minimum Drag, SAE Paper No. 760186, Feb. 1976.

Nedley, Lloyd, An Effective Aerodynamic Program in the Design of a New Car, SAE Paper No. 790724, June 1979.

Pershing, B. (Aerospace Corp.), "The Influence of External Aerodynamics on Automotive System Design," 'Advances in Road Vehicle Aerodynamics', pp. 25-52, BHRA Fluid Engineering, 1973.

Pershing, Bernard, and Masaki, Mamoru, Estimation of Vehicle Aerodynamic Drag, EPA-46/3-76-025, Oct. 1976.

Porter, F.C., Design for Fuel Economy--The New GM Front Drive Cars, SAE Paper No. 790721, June 1979.

Richie, D., "Beat the Built-In Head Wind," Commercial Car Journ., Sept. 1973.

Richie, D., "How to Beat the Built-In Head Wind," Owner-Operator, May/June 1973.

Romani, L., "La Mesure sur Piste de la Resistance a L'avancement," Road Vehicle Aerodynamics: Proc. First Symp., Paper 15, 12 pss, City University, London, Nov. 6-7, 1969.

Romberg, G.F., Chianese, F., Jr., and Lajoie, R.G., "Aerodynamics of Race Cars in Drafting and Passing Situations," Paper 710213, SAE Automotive Engineering Congress, Detroit, MI, Jan. 1971.

Saltzman, E.J., and Meyer, R.R., Jr., Drag Reduction Obtained by Rounding Vertical Corners on a Box-Shaped Ground Vehicle, NASA TM X-56023, Mar. 1974.

Saltzman, E.J., Meyer, R.R., Jr., and Lux, D.P., Drag Reductions Obtained by Modifying a Box-Shaped Ground Vehicle, NASA TM X-56027, Oct. 1974.

Schenkel, F.K., The Origins of Drag and Lift Reductions on Automobiles with Front and Rear Spoilers, SAE Paper No. 770389, Feb. 1977.

Schlicting, H., Aerodynamic Problems of Motor Cars, AGARD Report, 307, Oct. 1960.

Schmid, C., "Air Resistance of Automobiles," Technical University Stuttgart, VDI, Sept. 1938.

Schmid, C., "Lufwiderstand an Kraftfahrzeugen Versuche am Fahrzeug und Modell," VDI - Verlag, 1938.

Scibor-Rylski, A., (City Univ., U.K.), "Experimental Investigation of the Negative Aerodynamic Lift Wings Used on Racing Cars," 'Advances in Road Vehicle Aerodynamics' 1973, p. 147-154, BHRA Fluid Engineering, 1973.

Shapiro, A., Shape and Flow - The Fluid Dynamics of Drag, Science Study Series, Anchor Books, Doubleday and Co.

Smalley, W.M., and Lee, W.B., Assessment of an Empirical Technique for Estimating Vehicle Aerodynamic Drag from Vehicle Shape Parameters", Aerospace Rept. No. ATR-78 (7623-03)-1, July 1978.

Stafford, L.G. (City Univ., U.K.), "A Numerical Method for the Calculation of Flow Around a Motor Vehicle," 'Advances in Road Vehicle Aerodynamics' 1973, p. 167-183, BHRA Fluid Engineering, 1973.

Stapleford, W.R., and Carr, G.W., Aerodynamic Characteristics of Exposed Rotating Wheels, MIRA Report No. 1970/2.

Tenniswood, D.M., and Graetzel, H.A., Minimum Road Load for Electric Cars, SAE Paper No. 670177, Detroit, MI, Jan. 1967.

Tustin, R.C., and Carr, G.W., Aerodynamics of Basic Shapes for Small Saloon Cars, MIRA Rept. No. 1965/7.

Tustin, R.C., and Carr, G.W., Aerodynamics of Basic Shapes for Small Saloon Cars, MIRA Rept. 1963/10, p. 23.

Yoshiyvki, K., et al., Datsun 280 ZX - Integration of Aerodynamics and Appearance, SAE Paper No. 800141, Detroit, MI, 1980.

B. FACILITY TESTING

Antonucci, G., Ceronetti, G., and Costelli, A., Aerodynamic and Climatic Wind Tunnels in the Fiat Research Center, SAE Paper No. 770392, Feb. 1977.

Barth, R., Wind Tunnel Measurements on Vehicle Models and Rectangular Bodies with Different Proportions in Unsymmetrical Flow, Technischen Hoechschule Stuttgart Thesis (in German), 1958.

Beauvais, F.N., Trignor, S.C., and Turner, T.R., "Accuracy of Car Wind Tunnel Tests Not Aided by Moving Ground Plane," SAE Journ., Vol. 77, No. 9, pp. 64-67, 1969.

Beauvais, F.N., Turner, T.R., and Tignor, S.C., "Problems of Ground Simulation in Automobile Aerodynamics," SAE Paper No. 680121, Jan. 1968.

Bettes, W.H., "Aerodynamic Testing of High Performance Land-Born Vehicles - A Critical Review," in AIAA Symposium on the Aerodynamics of Sports and Competition Automobiles, Los Angeles, CA, Apr. 1968.

Bettes, W.H., and Kelly, K.B., "The Influence of Wind Tunnel Solid Boundaries on Automotive Test Data," 'Advances in Road Vehicle Aerodynamics' 1973, p. 271-290, BHRA Fluid Engineering, 1973.

Brown, G.J., and Seeman, G.R., The Highway Aerodynamic Test Facility, AIAA Paper 72-1000, Sept. 1972, also 'Advances in Motor Vehicle Aerodynamics', 1973, pp.323-333, BHRA Fluid Engineering, 1973.

Buchheim, R., et al., Comparison Tests Between Major European Automotive Wind Tunnels, SAE Paper No. 800140, Detroit, MI, 1980.

Carr, G.W., Aerodynamic Effects of Underbody Details on a Typical Car Model, MIRA Rept. No. 1965/7.

Carr, G.W., The MIRA Quarter-Scale Wind Tunnel, MIRA Report No. 1961/11.

Carr, G.W., Correlation of Pressure Measurements in Model - and Full-Scale Wind Tunnels and on the Road, SAE Paper No. 750065, Feb. 1975.

Cogotti, A., et al., Comparison Tests Between Some Full-Scale European Automotive Wind Tunnels - Pininfarina Reference Car, SAE Paper No. 800139, Detroit, MI, 1980.

Doberenz, M.E., and Selberg, B.P., A Parametric Investigation of the Validity of 1/25 Scale Automobile Aerodynamic Testing, SAE Paper No. 760189, Feb. 1976.

Fosberry, R.A.C., White, R.G.S., and Carr, G.W., A British Automotive Wind Tunnel Installation and Its Application, SAE Paper 948C, Jan. 11-15, 1965.

Fosberry, R.A.C., and White, R.G.S., A 250 hp Chassis Synamometer, MIRA Rept. No. 1963/9.

Fosberry, R.A.C., and White, R.G.S., The MIRA Full-Scale Wind Tunnel, MIRA Rept. No. 1961/8.

Fosberry, R.A.C., and White, R.G.S., A Wind Tunnel for Full-Scale Motor Vehicles - Design Investigation with 1/24 Scale Model, MIRA Rept. 1960/2, 24 p.

Gross, D.S., and Sekscienski, W.S., Some Problems Concerning Wind Tunnel Testing of Automotive Vehicles, SAE Paper 660385, 1966.

Hensel, R.W., Rectangular-Wind Tunnel Blocking Corrections Using the Velocity-Ratio Method, TN2372, NACA, June 1951.

Kamm, W., and Schmid, C., Automobile Testing, Julius Spring, Berlin, 1938.

Kessler, J.C., and Wallis, S.B., Aerodynamic Test Techniques, SAE Detroit Section Jr. Activity, No. 660464, Feb. 1966.

Larrabee, E.E., Small Scale Research in Automobile Aerodynamics, SAE Preprint 660384, June 1966.

Mason, W.T., and Sovran, G. (G.M), "Ground-Plane Effects on the Aerodynamic Characteristics of Automobile Models - An Examination of Wind Tunnel Test Techniques," 'Advances in Motor Vehicle Aerodynamics' 1973, pp. 291-309, BHRA Fluid Engineering, 1973.

Mason, W.T., and Sovran, G., Ground Plane Effects on Vehicle Testing, General Motors Research Publication GMR-1378.

Metz, L.D.. and Sensenbrenner, K. (Univ. of Ill.)(N.A.R. Corp.), The Influence of Roughness Elements on Laminar to Turbulent Boundary Layer Transition as Applied to Scale Model Testing of Automobiles, SAE Paper 730233.

Moller, E., "Wind Tunnel Measurements on Automobiles in a Cross Wind," ATZ, Vol. 53, No. 4, p. 74 (in German), Apr. 1951.

Morelli, A. (Italy), "The New Pininfarino Wind Tunnel for Full-Scale Automobile Testing," Advances in Road Vehicle Aerodynamics, 1973.

Muto, Shinri, and Ashihara, Tomo-o, The J.A.R.I. Full-Scale Wind Tunnel, SAE Paper No. 780336, Feb. 1978.

Oda, Norihiko, and Hoshino, Teruo, Three Dimensional Airflow Visualization by Smoke Tunnel, SAE Paper No. 741029, Oct. 1974.

Ohtani, K., Takei, M., and Sakamoto, H., Nissan Full-Scale Wind Tunnel - Its Application to Passenger Car Design, SAE Preprint 720100, Automotive Engineering Congress, Detroit, MI, Jan. 10-14, 1972.

Sykes, D.M. (City Univ., U.K.), "Blockage Corrections for Large Bluff Bodies in Wind Tunnels," Advances in Motor Vehicle Aerodynamics, 1973.

Turner, T.R., Wind Tunnel Investigations of a 3/8 Scale Automobile Model over a Moving-Belt Ground Plane, NASA Tech. Note TN D-4229, Nov. 1967.

Turner, T.R., A Moving-Belt Ground Plane for Wind-Tunnel Ground Simulation and Results for Two Jet-Flap Configuration, NASA TN D-4228, 1967.

C. ROAD TESTING

Fuel Economy Measurement - Road Test Procedure, SAE J1082 (SAE Recommended Practice - Apr. 1974).

Brennand, J., Electric Vehicle Tire and Aerodynamic Friction, Road Power, and Motor-Driveline Efficiency from Track Tests, SAE Paper No. 780218, Feb. 1978.

Buckley, B.S., Road Test Aerodynamic Instrumentation, SAE Paper No. 741030, Oct. 1974.

Yasin, T.P., The Analytical Basis of Automobile Coastdown Testing, SAE Paper No. 780334, Feb. 1978.

A Digital Technique for the Measurement of Total Drag Deceleration of a Vehicle, MIRA Bulletin No. 1, pp. 1420, 1959.

Carr, G.W., and Rose, J.J., Correlation of Full-Scale Wind Tunnel and Road Measurements of Aerodynamic Drag, MIRA Rept. No. 1964/5.

Cray, R.A., Digital Acceleration Equipment, MIRA Bulletin No. 1, pp. 11-14, 1963.

Dayman, B., Jr., Tire Rolling Resistance Measurements From Coast-Down Tests, SAE Paper No. 760153, Feb. 1976.

Fosberry, R.A.C., and Holubecki, Z., The Aerodynamics of Road Vehicles - Road Measurements of Drag and Comparison with Wind Tunnel Measurements, MIRA Rept. 1958/10, 11 p.

Fosberry, R.A.C., and White, R.G.S., The Aerodynamics of Road Vehicles - A Comparison of Cars and Their Models in Wind Tunnels, MIRA Rept. 1958/9, 37 p.

Hoerner, S.F., "Determination de la Resistance Aerodynamique des Vehicules par la Methode Roue Libre," (Determination of the Aerodynamic Resistance of Vehicles by the Coastdown Method), ZVDI 79 No. 34, pp. 1028-33, Aug. 1935.

Klein, R.H., and Jex, H.R., Development and Calibration of an Aerodynamic Disturbance Test Facility, SAE Paper No. 800143, Detroit, MI, 1980.

Korst, H.H., and White, R.A., "Aerodynamic & Rolling Resistances of Vehicles as Obtained from Coast-Down Experiments," 2nd International Conf. on Vehicle Mechanics, Paris, Sept. 1971.

Larrabee, E.E., "Measuring Car Drag," Road and Track, Vol. 12, No. 6, pp. 24-28.

Lucas, G.G., and Britton, J.D., "Drag Data from Deceleration Tests and Speed Measurements During Vehicle Testing," Proc. of the 1st Road Vehicle Aerodynamics Symposium, City Univ., London, Nov. 1969.

Ordorica, M.A., "Vehicle Performance Prediction," SAE Paper 650623, May 1965, and SAE Journ., Vol. 74, No. 1, pp. 101-104, Jan. 1966.

Rousilion, G., Marzin, J., and Bourhis, J. (Peugeot), "Contribution to the Accurate Measurement of Aerodynamic Drag by the Deceleration Method," 'Advances in Road Vehicle Aerodynamics' 1973, pp. 53-66, BHRA Fluid Engineering, 1973.

Saltzman, E.J., and Meyer, R.R., Jr., Drag Reduction Obtained by Rounding Vertical Corners on a Box-Shaped Ground Vehicle, NASA TM X-56023, Mar. 1974.

Walston, W.H., Jr., Buckley, F.T., Jr., and Marks, C.H., Test Procedures for the Evaluation of Aerodynamic Drag on Full-Scale Vehicles in Windy Environments, SAE Paper No. 760106, Feb. 1976.

White, J.F., New Techniques for Full-Scale Testing, SAE Preprint No. 148E, SAE National Automobile Meeting, Detroit, MI, Mar. 1960.

White, R.A., and Korst, H.H., The Determination of Vehicle Drag Contributions from Coast-Down Tests, SAE Paper 720099, 1972. Also, 'Advances in Road Vehicle Aerodynamics' 1973, pp. 15-23, BHRA Fluid Engineering, 1973.

Schmid, C., "Aerodynamic Drag of Motor Vehicles: Experiments with Full-Scale Car and Model," Deutsche Kraftfahrforschung, No. 1, 1938, VDI Verlag (in German).

Sherman, D., "Project Car: Crisis-Fighter Z-Car," Car and Driver, May 1974.

Sherman, D., "Project Car: Crisis-Fighter Pinto," Car and Driver, Mar. 1974.

Sturm, J.M., Acceleration and Fuel Measurements - New Tools and Techniques, SAE Paper 471G, Jan. 1972.

D. WIND NOISE

McDaniel, D.W., Hushing Automobile Noises, SAE Preprint No. 477A, Automotive Engineering Congress, Detroit, Jan. 1972.

Richardson, E.J., Isolation and Cure of Wind Noises, SAE Special Publication 195, pp. 14-31, Feb. 1961.

Oswald, L.J., and Dolby, D.A., A Technique for Measuring Interior Wind Rush Noise at the Clay Model Stage of Design, SAE Paper No. 770394, Feb. 1977.

Romberg, G.F., and Lajoie, R.G., An Objective Method of Estimating Car Interior Aerodynamic Noise, SAE Paper No. 770513, Feb. 1977.

Wattanabe, Masaru, Harita, Mituyuki, and Hayashi, Eizo, The Effects of Body Shapes on Wind Noise, SAE Paper No. 780266, Feb. 1978.

E. VENTILATION AND ENGINE COOLING

Davenport, C.J., Beard, R.A., and Scott, P.A.J., Optimization of Vehicle Cooling Systems, SAE Paper No. 740089, Feb. 1974.

Emmenthal, K.D., and Hucho, W.H., A Rational Approach to Automotive Radiator Systems Design, SAE Paper No. 740088, Feb. 1974.

Fogg, A. and Brown, J.S., Some Experiments on Scale-Model Vehicles with Particular Reference to Dust Entry, MIRA Report 1948/1.

Goetz, Hans, The Influence of Wind Tunnel Tests on Body Design, Ventilation, and Surface Deposits of Sedans and Sport Cars, SAE Paper No. 710212, Feb. 1971.

Olson, M.E., Aerodynamic Effects of Front End Design on Automobile Engine Cooling Systems, SAE Paper No. 760188, Feb. 1976.

Paish, M.G., and Stapleford, W.R., "A Rational Approach to the Aerodynamics of Engine Cooling System Design", 1968-69 Proceedings of the Institution of Mechanical Engineers, Automobile Division, Vol. 183, Part 2A, Number 3, England.

Paish, M.G., Airflow Measurement Through Vehicle Cooling Systems," MIRA Bulletin No. 6, 1966.

Paish, M.G. and Stapleford, W.R., A Study to Improve the Aerodynamics of Vehicle Cooling Systems, MIRA Report 1968/4.

Taylor, G. I., Air Resistance of a Flat Plate of Very Porous Material, British Aeronaut. Research Council Rept. and Mem 2236, 1944.

Wallis, S.B., Ventilation System Aerodynamics - A New Design Method, SAE Paper No. 710036, Feb. 1971.

F. STABILITY AND HANDLING

Basso, G.L., Functional Derivation of Vehicle Parameters for Dynamic Studies, National Aeronautical Establishment LTR-ST. 47, Ottawa, Canada, Sept. 1974.

Hawks, R.J., The Effect of Aerodynamic Forces on the Performance and Handling Qualities of High-Speed Automobiles, Ph.D. Dissertation, Univ. of Maryland, Jan. 1972.

Hawks, R.J., and Larrabee, E.E., "The Calculated Effect of Cross Wind Gradients on the Disturbance of Automobile Vehicles," presented at AIAA Symposium on the Aerodynamics of Sports and Competition Automobiles, Los Angeles, CA, Apr. 1968.

Korff, W.H., "The Aerodynamic Design of the Goldenrod to Increase Stability, Traction and Speed," presented at AIAA Symposium on the Aerodynamics of Sports and Competition Automobiles, Los Angeles, CA, Apr. 1968.

Lay, W.E., and Letts, P.W., "Wind Effects on Car Stability," SAE Transactions, Vol. 61, p. 608, 1953.

Mahig, J. (Univ. of Fla.), "Variation in Vehicle Handling Characteristics Under Gusty Conditions," Advances in Road Vehicle Aerodynamics, 1973.

Moncarz, H.J., Barlow, J.B., and Hawks, R.J. (Univ. of MD), "Stability and Cross-Wind Response of an Articulated Vehicle with Roll Freedom," Advances in Road Vehicle Aerodynamics, 1973.

Weir, P.H., Heffley, R.K., and Ringland, R.F., "Simulation Investigation of Driver/Vehicle Performance in a Highway Gust Environment," 8th Annual Conference on Manual Control, May 1972.

G. GENERAL BOOKS AND PROCEEDINGS

Vehicle Dynamics Terminology, SAE J67d, SAE Handbook Supplement J671, published 1965.

Bekker, M.G., Theory of Land Locomotion, University of Michigan Press, Ann Arbor, MI, 1956.

Bussien, R. (editor), Automobiltechnisches Handbuch, Technischer Verlag, Herbert Cram, Berlin, 1942.

Hayes, M.R., and Bannister, B., Auto Union Audi Saloon Car, MIRA Rept. No. V.A. 21, 21 p., 1963.

Kamm, W., Das Kraftfahrzeug (The Motor Vehicle).

Whitelaw, R.L., "Three Imperatives in the Automobile Future," Proceedings of the Second International Conf. on Vehicle Mechanics, Paris VI University, Sept. 1971.

Aerodynamic Drag Mechanisms of Bluff Bodies and Road Vehicles, GM Symposium, Sept. 1976, edited by Gino Sovran, Thomas Morel, and William Rason. Plenum Press, 1978.

Aerodynamics of Sports and Competition Automobiles, edited by Bernard Pershing, AIAA Symposium, May 1974.

"Aerodynamics of Transportation," edited by Thomas Morel and Charles Dalton, Proceedings of ASME Symposium Held June 1979, Niagara Falls, NY

Advances in Road Vehicle Aerodynamics, 1973, edited by H.S. Stephens, BHRA Fluid Engineering, 1973.

Automotive Aerodynamics, SAE/PT-78/16 (selected SAE Papers through 1977).

"Road-Vehicle-Aerodynamics", edited by Carl Kramer and Hans J. Gerhardt, Proceedings of the 4th Colloquium on Industrial Aerodynamics, Aachen, W. Germany, June 1980.

APPENDIX A

EFFECTS OF ASPECT RATIO AND FINENESS RATIO ON THE AERODYNAMIC CHARACTERISTICS OF AUTOMOBILE SHAPES

Because of their special battery packaging requirements, electric vehicles may not be subject to the same design constraints as conventional IC engine vehicles. For instance, owing to the use of a central battery tunnel, a small vehicle may be unusually wide or long. A series of tests was therefore performed in the GALCIT 10 foot wind tunnel (Caltech) to determine if aspect ratio or fineness ratio[1] was an important aerodynamic parameter, and further, whether one can generalize the effect of either or both in combination for simplified automobile shapes.

These tests were exploratory in nature and intended to determine what, if any, trends would appear. The initial tests involved both a sharp-edged and a round-edged basic model (Figures A-1 and A-2), in order to quantify the effect of local flow separation on the observed aerodynamic trends.

The parameters varied were height, length, width, and ground clearance; Figure A-3 illustrates the model construction technique. Three variations were available for each of the four parameters. Figure A-4 illustrates the drag trends demonstrated by highly separated (sharp-edged model) and highly attached (round-edged model) flow situations at low to moderate fineness ratios. As one might expect, for very short vehicles, the drag is reduced with increasing fineness ratio. This is probably due to a reduction in the form drag component (see Appendix B, Part B) at the expense of a small increase in surface friction drag. Owing to local separation points, the drag gradient is not as large for the sharp-edged model as for the round-edged, but the trend is not significantly different. Subsequent tests involved only the round-edged model.

The effects of ground clearance were found to be significant with these smooth-underbody models (see Figure A-5). This also presents a problem in data presentation since the manner by which the ground clearance is nondimensionalized can distort the effects of aspect and fineness ratios. For instance, if the ground clearance is nondimensionalized by body width and the aspect ratio is varied by changes in body width (g/W) ground clearance changes <u>with</u> aspect ratio and dominates the whole effect. Similarly, ground clearance nondimensionalized by body length (g/L) will dominate the effects of changes in fineness ratio. For these reasons, two ground clearance parameters, g/L and g/W, are used when evaluating the effects of aspect and fineness ratios, respectively.

---

[1]Aspect ratio (AR) is defined as body height (not including ground clearance) divided by width, and fineness ratio (FR) as length divided by effective diameter (of equivalent area circle).

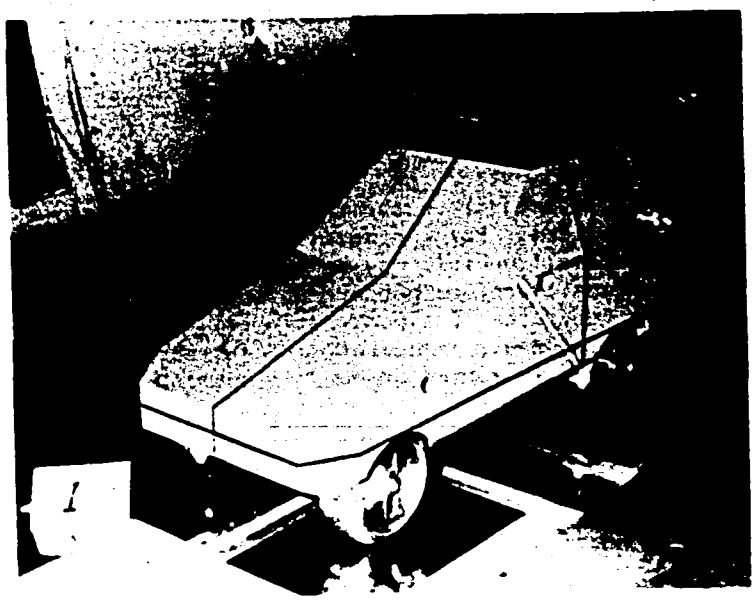

Figure A-1. Basic Sharp-Edged Model Mounted in GALCIT Wind Tunnel

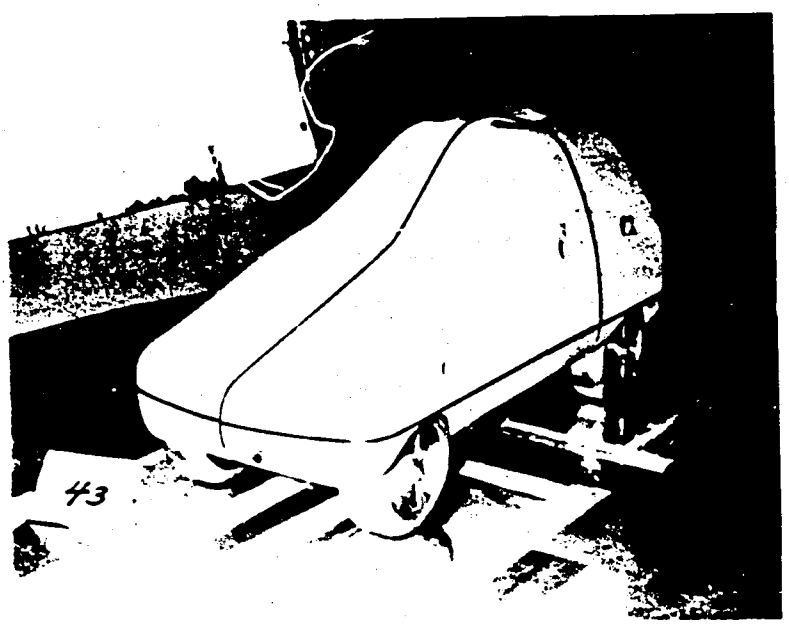

Figure A-2. Basic Round-Edged Model Mounted in GALCIT Wind Tunnel

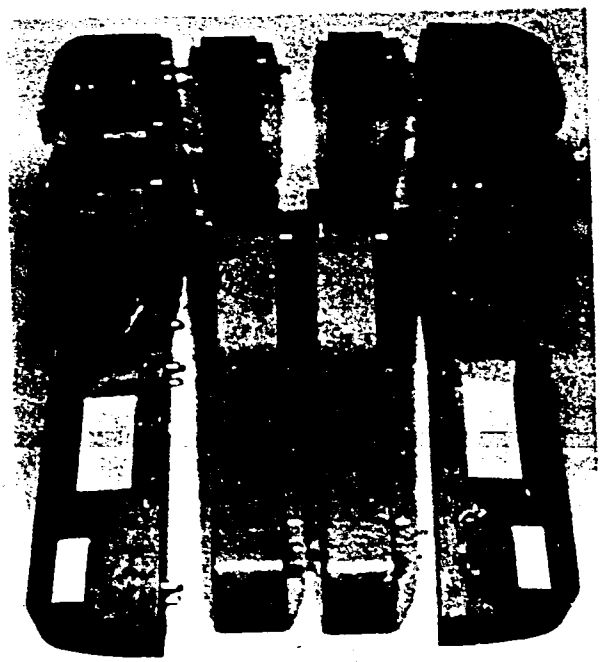

Figure A-3. Some of the 56 Pieces Used to Alter Aspect and Fineness Ratios

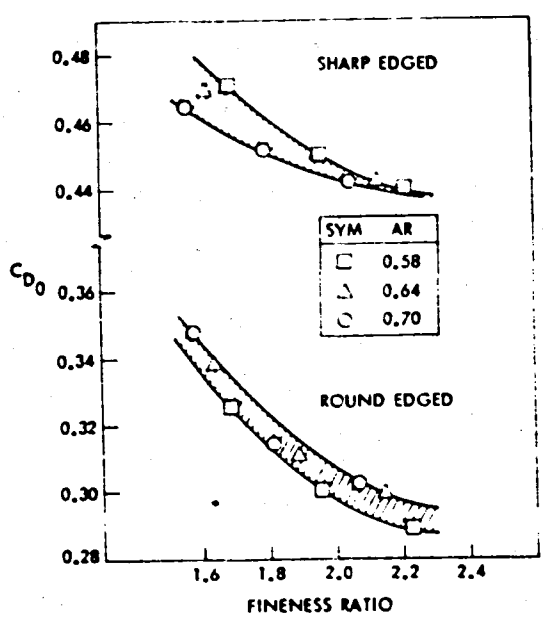

Figure A-4. Drag Coefficient vs. Fineness Ratio for Sharp-Edged and Round-Edged Automobile Shapes (g/W = 0.15, Ground Clearance = 15% of Body Width)

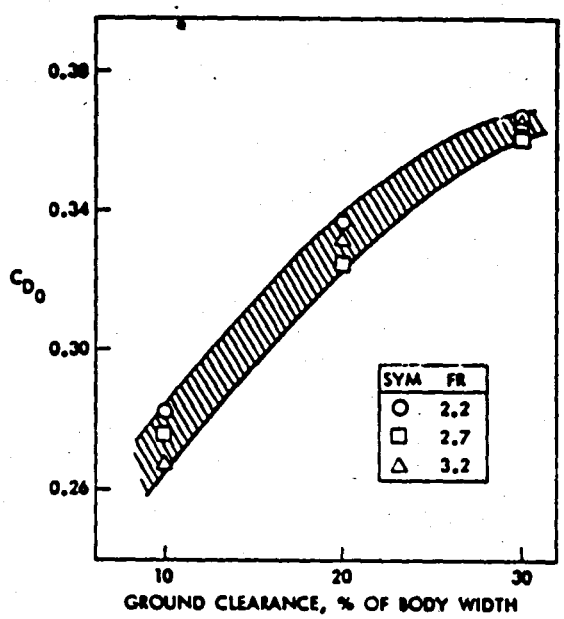

Figure A-5. Drag vs. Ground Clearance (Aspect Ratio = 0.88)

The effect of aspect ratio on drag is shown in Figure A-6 at two levels of ground clearance representative of present day automobiles (g/L = 5%) and vans (g/L = 8%). In both cases, the drag usually increases with aspect ratio (short and wide has some advantages over tall and narrow), being more pronounced at the highest fineness ratio (longest vehicle). For high-ground-clearance vehicles, there seems to be a weak aspect ratio effect up to about AR = 0.8; beyond that point, the drag increases significantly.

The effect of fineness ratio (Figure A-7) is a little more confusing in that the trends with constant aspect ratios are not as internally consistent. Note also, that the two ground clearances representing "automotive (g/W = 10%) and van-like (g/W = 20%)" are nondimensionalized by body width for the reasons explained earlier. In general, the trend is consistent with Figure A-4 which covered the very low fineness-ratio end of the spectrum. However, as the fineness ratio is increased, significant drag reduction ceases and the drag actually begins to increase beyond a fineness ratio of 2.7 at the higher ground clearance. This may indeed be the result of a rapid buildup of the surface friction drag component (see Appendix B, Part B), which may be magnified in the underbody region at high ground clearances.

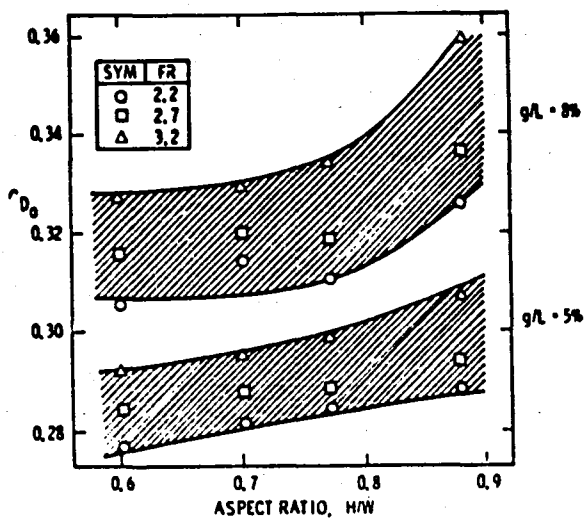

Figure A-6. Drag vs. Aspect Ratio at Two Ground Clearances

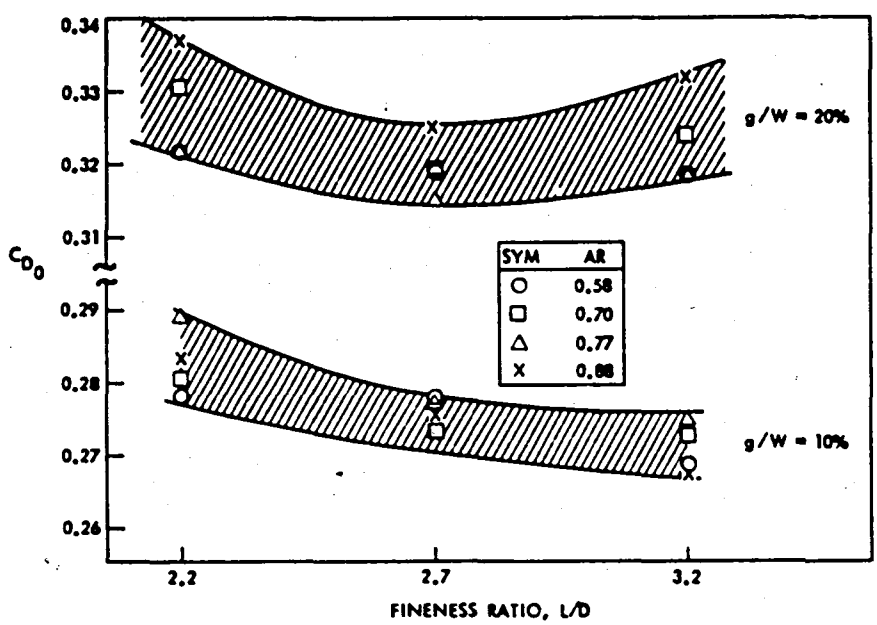

Figure A-7. Drag vs. Fineness Ratio at Two Ground Clearances

In summary, these results indicate that there are aspect and fineness ratio effects on vehicle drag that warrant consideration during initial design stages when packaging requirements are being developed.

APPENDIX B

FOUNDATIONS OF AERODYNAMIC DESIGN

The purpose of this section is to familiarize the EHV design engineer with certain basic concepts related to automotive aerodynamics. First, the historical development of the automobile, from an aerodynamic perspective, is briefly reviewed. Next, the generally accepted "sources of drag" are identified, ranked by importance and described by example. Finally, a limited aerodynamic data base, developed by wind tunnel testing 20 electric, hybrid and subcompact vehicles, is presented in order to orient the design engineer with the state of the art.

A. HISTORICAL DEVELOPMENT

Although many of the principles involved in low-drag designs have long been known, the drag coefficient of the average production car in the early 1920s was about 0.8. By 1940 it had dropped to about 0.6 and by 1960 to about 0.5 (see Figure B-1). Further improvement has come slowly, especially in this country, and the average drag coefficient of domestic automobiles actually increased slightly (to about 0.55) in recent years with the trend toward more formal styling with less rounding of edges. Most recently, however, the pressures brought by federally mandated fuel economy requirements have sparked renewed interest in reducing aerodynamic losses. In Europe, the current average production car drag coefficient is somewhat lower, about 0.46. Drag coefficients as low as 0.15 were reported as early as 1922 by W. Klemperer (Reference B-1) on an elongated tear-drop automobile model. A. Morelli in 1976 (Reference 3-5) developed (in full-scale mock-up) a body shape encompassing reasonable four-passenger compartment and engine cooling airflow with a drag coefficient of 0.172. Daimler-Benz recently unveiled the new experimental Mercedes C-111/3, a turbodiesel which set several speed records and is reported to have a drag coefficient of 0.195 (Reference B-2). Perhaps the lowest recorded drag coefficient for a real ground vehicle is 0.12 for the Goldenrod, which holds the land speed record for wheel-driven vehicles (Reference B-3). It appears, then, that there exists a rather large gap between the drag level of today's automobile and what is theoretically possible as demonstrated by some of these very specialized vehicles. Obviously, there are many practical constraints on production automobiles which compromise efforts to achieve low drag levels. However, the hope of eventually cutting present-day production car drag levels nearly in half may not be completely unrealistic.

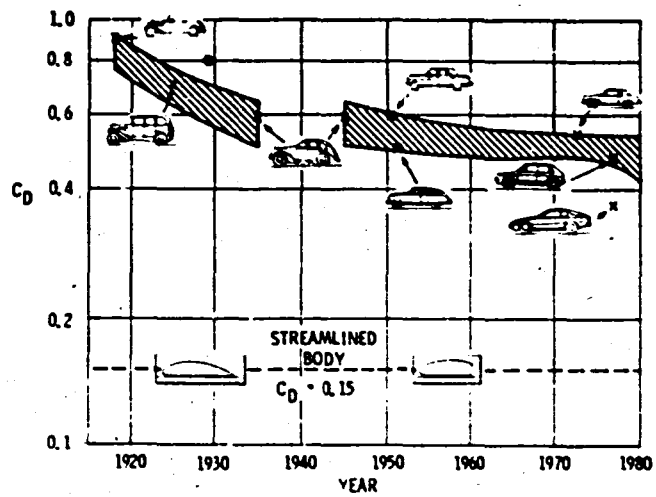

Figure B-1. Aerodynamic Drag of Cars as a Function of Time

B. SOURCES OF DRAG

The actual mechanisms of automotive drag production are not at all well understood. Automotive aerodynamics is characterized by ground interference and large areas of separated and vortex flow. Unlike aircraft aerodynamics it is largely unresponsive to classical analytical treatment. It has therefore become a rather empirical science, relying heavily on development through wind tunnel test techniques. Reference B-4 and others break down the sources of drag into five basic categories: (1) form drag, (2) interference drag, (3) internal flow drag, (4) surface friction drag, and (5) induced drag. A simple schematic depicting their relative importance for an IC engine car is presented in Figure B-2.

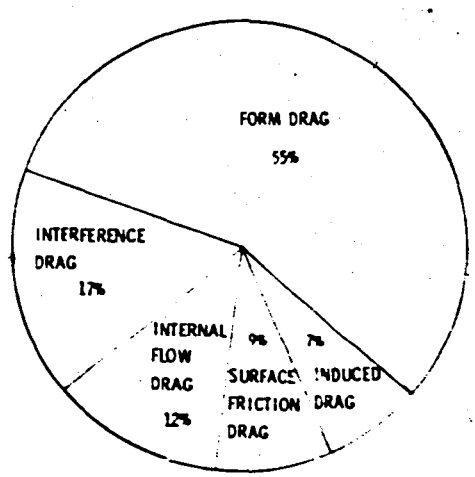

Figure B-2. Distribution of IC Engine Vehicle Aerodynamic Drag (Reference B-4)

Form drag (sometimes called profile drag) is a function of the basic body shape. Bodies which minimize the positive pressure on the nose and the negative pressure on the tail will exhibit lower form drag. For example, a flat plate positioned normal to the flow would represent a worst case, whereas a streamlined teardrop shape would be characteristic of minimum form drag.

Interference drag develops as the flow over the many exterior appendages of a vehicle body interacts with the flow over the basic shape or the flow due to the constraining influence of the ground. Various component projections such as a hood ornament, windshield wipers, radio antenna, external mirrors, door handles, luggage rack, rain gutters, and underbody protuberances all contribute to the interference drag component. For example (Reference B-4), an external mirror in a free airstream may have a drag force of 4 newtons. In close proximity to the vehicle body where the local airflow is accelerated by 25-30%, the drag on the mirror may be 6.4 newtons --a 60% increase! Since an external mirror usually has a large flat aft end, it spreads a turbulent wake behind it which disturbs the basic flow on the side of the vehicle, adding a further drag increment. Projecting elements usually cause less interference on high-drag body shapes than on low-drag bodies. Since a high-drag body is usually characterized by extensive regions of separated flow, many of these elements are hidden in the already disturbed flow pattern. Conversely, the low drag of an efficient body is the result of a high degree of flow attachment. That condition is usually tenuous and any projection from the surface may cause separation. The underbody projections are some of the prime offenders as the installation of a smooth belly pan has demonstrated many times (Reference 3-8). In the case of electric vehicles the traditional arguments against using a smooth belly pan--such as ease of maintenance, safety (oil drippings, etc.), and engine cooling restrictions--may not apply.

Internal flow drag arises because air is required to move through the vehicle as well as around it. A conventional water-cooled IC engine requires a substantial amount of radiator airflow. Typically, the flow path is highly inefficient as local stagnation areas develop in the engine compartment and the exit path is filled with struts, hoses, brackets, and suspension elements. Here again, an electric vehicle may have an inherent advantage since its cooling requirement may be an order of magnitude less. However, ventilation of the passenger compartment is an important comfort and noise consideration, and care must be taken to design and locate the inlets and exits properly. The conventional approach is to place a flush inlet in a relatively high pressure region (usually at the base of the windshield) and either place exits in a low pressure region around the rear window or rely on normal body leaks. Unless a scoop is placed out in the flow (in which case there is an interference drag component), the drag increment due to normal occupant ventilation requirements is negligible.

Surface friction drag results from the boundary layer which is formed as air moves along a surface. Owing to viscous friction forces, the velocity gradient normal to the surface gives rise to a shear layer. The surface finish or small imperfections, and the size of the area exposed to the flow, determine the level of this drag component. Production car finishes (surface grain size of 0.2 to 0.5 mils) are well below the critical level where additional smoothness would reduce the local friction. A smooth, continuous surface keeps skin friction low. As the flow moves rearward along a body it continually loses energy and separation is more likely to occur in critical areas. Window frames, gaps, mismatched parts, and normal skin friction all contribute to cause a buildup of the boundary layer, leading to separation, more turbulence and increased drag.

Induced drag arises from the formation of longitudinal trailing vortices generated by the pressure differential between the vehicle's underbody and roof. The energy required to generate and support this vortex field is related to the energy consumed by induced drag. Often termed "lift-induced" drag or drag due to lift, there is now real doubt that any simple relationship between lift and induced drag exists (Reference 3-4). It can normally be minimized by careful attention to design detail on the rear portions of the vehicle, but this usually requires an experimental approach.

C. AERODYNAMIC DATA BASE

Very little reliable aerodynamic data on conventional automobiles and virtually none on special electric or hybrid vehicles is available in the public domain. The automobile manufacturers, both foreign and domestic, have generated a great deal of aerodynamic information for IC engine vehicles but it remains largely proprietary. Most of the available data is from subscale wind tunnel tets of questionable or unknown origin. Here lies a basic problem with random wind tunnel data: it is usually not reliable nor directly comparable to other test results. Owing to such factors as scale, level of detail (internal flow paths, undercarriage, etc.) flow conditions, and data reduction procedures, the absolute values of the coefficients are of limited value. The difference in measured drag between a "reasonably detailed" scale model and the full-sized production vehicle is often 20% or greater. The same automobile tested in two different wind tunnels may yield drag results which differ by 10%. The various tunnel wall corrections alone can modify the drag by 10%. To maximize its usefulness, a data base must be generated at the same model scale, in the same wind tunnel under the same conditions, and be handled using identical data reduction procedures. The relative effects represented by the data base should then be sufficiently reliable for design use. Correlations with road test results can help to establish a confidence level for the absolute values.

With this background in mind, it was determined that the development of an EHV aerodynamic data base should be initiated by performing full-scale tests in the Lockheed-Georgia Low-Speed Wind

Tunnel. A Request for Quotation (RFQ) was prepared and sent to 25 owners or developers of electric or hybrid vehicles asking for the use of a vehicle for aerodynamic characterization testing during a specific time period. Nine bids were received before the RFQ closing date. Among the selection criteria used were:

(1) Availability.

(2) Compatibility with wind tunnel balance system.

(3) Aerodynamic interest.

(4) Loan and transportation fees.

Four vehicles were selected by this process. In addition, three electric vehicles were loaned by the NASA Lewis Research Center. One was loaned by South Coast Technology and three were available at JPL. To supplement the group, several conventional IC subcompacts were borrowed from local dealerships and individuals. In three cases, a facsimile of an IC engine/EHV conversion was substituted.

These vehicles are described in Table B-1 and shown in Figure B-3. Forty-eight vehicle configurations were investigated in the course of the testing to quantify the effects of such things as open windows, attitude changes (due to loading) and pop-up headlights (References 2-1 and 3-10 contain more detailed information on this as well as the other aerodynamic force and moment components). The zero-yaw drag coefficients of all 20 vehicles in their "standard" configurations, their frontal areas and drag-area products are also included in Figure B-3. When the yaw characteristics are considered (effects of ambient winds), the relative values change slightly (Reference 2-1). See Appendix F.

The vehicles were mounted on the external balance by means of a four-point support system. No attachment was required; the wheels merely rested on the four pads with the parking brakes locked. The friction between the tires and the pads was normally sufficient to maintain model position. In certain cases, chocks were placed behind the tires. Because of the extremely short wheelbases of some of these electric vehicles, it was necessary to use pad extensions. These raised the position of the vehicle in the tunnel by approximately 3 centimeters. To quantify the effect of this position change, tests were made using spacers with a few of the vehicles that were capable of using the unmodified pads. Elevating a vehicle in this manner appeared to increase the measured drag by 1-2% over the entire yaw range.

All tests were performed at 88 kph and the yaw angle (ψ) was varied through ± 40 degrees. Runs were also made on all vehicles with the two front windows open. Some tests of IC engine cars were run with radiators both open and blocked.

D. OBSERVATIONS

It is difficult to make universal statements about the data since, in automotive aerodynamics, broad generalizations usually prove to be unreliable. There are many subtle details characteristic of each vehicle which affect the local flow conditions and hence, the forces and moments. To state that vehicles of a particular class all exhibit predictable aerodynamic traits is risky at best. Nevertheless, certain features characteristic of this data base will be highlighted in what follows. In addition, a simplified procedure for accurately determining the effects of statistically varying ambient winds on a vehicle's drag is presented (and applied to this data base) in Appendix F.

Drag

It is interesting to note that the selected vehicles represent a range of zero-yaw drag coefficients from 0.308 to 0.583. Further, the highest value (least aerodynamically efficient) of the group was the Kaylor open roadster followed closely by the boxey Otis van; however, the HEVAN drag coefficient was nearly 15% less at 0.497 despite its boxey lines. Another interesting result was that the Horizon's drag coefficient was over 18% lower than the Chevette's even though they are very similar in shape[1].

General Electric's ETV-1 and Centennial have drag valves significantly lower than the rest of the group--a probable result of the importance of aerodynamics in the design theme and subscale wind tunnel testing.

Windows Open/Closed

Because of their current limited energy capacity, electric vehicles will not immediately be able to afford the luxury of an active air conditioning system; it is therefore reasonable to expect that they will be operated in a windows-open configuration over a significant portion of their lifetime. As previously discussed, open windows adversely affect the slope and ultimate magnitude of the drag-yaw curves. Curiously, open windows may or may not increase the drag at zero-yaw angle. In fact, four vehicles (Honda Civic Sedan and Wagon, HEVAN, and the Chevrolet Corvette) actually had a lower zero-yaw drag with their front windows open than when closed (almost 4% lower on the Civic wagon). This situation was previously observed while performing precision coast-down testing on a 1975 Chevrolet Impala (Reference 3-8). Although they reported this result, the authors were uncomfortable with it, and desired further investigation. The present data seems to confirm that the circumstance can and does occur. However, it should be noted that a vehicle operates at some angle of yaw (wind-induced) over most of its

---

[1]The relative drag levels of the cars tested in the Lockheed-Georgia wind tunnel must not be taken as typical of all their manufacturer's products.

lifetime; therefore, the effect of open window operation is a net increase in the vehicle's drag of approximately 3 to 5% (depending upon the driving cycle and wind speed - see Appendix F).

Ground Clearance

There is a natural boundary layer (velocity gradient) growth along the wind tunnel floor resulting in a thickness of about 15 cm (6 in.) at the test section midpoint for the Lockheed-Georgia wind tunnel. Since several of the short wheel base vehicles had to be mounted on raised/cantilevered plates (approximately 3 cm above the floor), a brief check was made to quantify the effect. The Chevette had a wheelbase length which made it possible to mount it either on the flush balance pads or on the cantilevered plates. Tests were performed in both positions with all other parameters unchanged. The effect of raising the vehicle was to increase the drag by from 1% to 2% over the entire yaw range. Certainly, one would expect there to be some increase since the vehicle is moving further out into the undisturbed freestream flow. It is believed that the effect observed with the Chevette is probably typical for the other vehicles tested on the cantilevered plates. It should be noted, however, that the data presented for these vehicles have not been corrected for this effect. The vehicles are: (1) Honda Civic Sedan, (2) Honda Civic Wagon, (3) Ford Fiesta (here the mounting procedure resulted in only a 1 1/2 cm elevation and the effect is expected to be less than 1%), (4) CDA Town Car, (5) Sebring-Vanguard Citicar, and (6) the Zagato Elcar.

Radiator Airflow

It has long been recognized that, for conventional automobiles, radiator airflow is a major source of aerodynamic drag. A great deal of effort has gone into developing designs which accomplish the engine cooling task while minimizing the detrimental aerodynamic effects (References B-5, B-6 and B-7). An all-electric vehicle, however, does not have a motor cooling requirement of similar magnitude and therefore should possess an inherent advantage in this respect. In an effort to quantify the benefit, two vehicles (the Chevette and the Corvette) were tested with their radiators both open to airflow and blocked. The blocking was accomplished by simply covering the grille, and other radiator inlet areas, with flexible sheet plastic held firmly in place with duct tape; all related body contours remained undisturbed. The Chevette with an open radiator exhibited about 7-8% higher drag than when the radiator was blocked. This increment was approximately constant across the yaw range, but the asymmetry was exaggerated with the open radiator. The Corvette had a 6 1/2% drag increase when open compared to blocked; this comparison, however, was made at zero yaw only. It is anticipated that the radiator drag increment might be different for each vehicle, and had time permitted, this would have been investigated. In summary, however, if an IC engine vehicle were converted to electric power and the radiator airflow were eliminated, one could expect a drag benefit of from 5 to 10%.

Table B-1. Data Base Vehicles

Figure	Vehicle	Type
a	General Electric Co.: ETV-1	4-passenger electric commuter
b	Garrett AiResearch Co.: ETV-1	4-passenger electric commuter
c	General Electric Co.: Centennial Electric	4-passenger electric commuter
d	Copper Development Association: Town Car	2-passenger electric commuter
e	South Coast Technology: Electric Rabbit	2-passenger electric commuter
f	Sebring-Vanguard: Citicar	2-passenger electric commuter
g	Zagato: Elcar	2-passenger electric commuter
h	Jet Industries: Electra Van 600	Electric delivery van
i	Otis Elevator Co.: Otis P-500A Van	Electric delivery van
j	Kaylor Energy Products: Kaylor GT	2-passenger hybrid-electric open roadster
k	Energy Research and Development Corp.: HEVAN (Hybrid Electric Van)	Hybrid-electric delivery van
l	American Motors Corp.: 1978 Pacer Station Wagon[1]	Internal combustion engine
m	American Motors Corp.: 1978 Pacer Sedan	Internal combustion engine
n	General Motors Corp.: 1967 Chevrolet Corvette[2]	Internal combustion engine
o	General Motors Corp.: 1978 Oldsmobile Delta 88[3]	Internal combustion engine
p	General Motors Corp.: 1978 Chevrolet Chevette 4-door	Internal combustion engine

q	Chrysler Corp.: 1978 Plymouth Horizon 4-door	Internal combustion engine
r	Honda Motors: 1978 Civic Sedan	Internal combustion engine
s	Honda Motors: 1978 Civic Wagon	Internal combustion engine
t	Ford Motor Co.: 1978 Fiesta	Internal combustion engine

Table Notes

[1]This production IC engine Pacer Wagon represented a reasonable facsimile of the Electric Vehicle Associates "Change of Pace" converted electric Pacer Wagon.

[2]This production IC engine Corvette represented a reasonable facsimile of the Cutler-Hammer Electric '67 Corvette of Santini. The front grille was blocked in order to eliminate the radiator losses, which are not present in the electric version.

[3]This production IC engine Delta 88 was a reasonable facsimile of the proposed National Motors Hybrid-Electric Gemini II. Here the radiator was not blocked since the hybrid vehicle would retain its V-6 engine and cooling system.

a.

GE ETV-1

C_{D_o}	A, m^2	$C_{D_o}A$, m^2
0.308	1.840	0.567

b.

Garrett ETV-2

C_{D_o}	A, m^2	$C_{D_o}A$, m^2
0.395	2.028	0.801

Figure B-3. Vehicles Tested in the Lockheed-Georgia Low-Speed Wind Tunnel

c.

GE Centennial

C_{D_o}	A, m^2	$C_{D_o}A$, m^2
0.337	1.851	0.624

d.

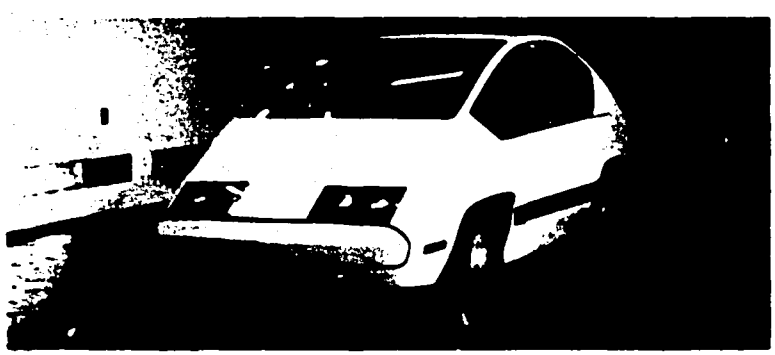

CDA Town Car

C_{D_o}	A, m^2	$C_{D_o}A$, m^2
0.367	1.754	0.644

Figure B-3. Vehicles Tested in the Lockheed-Georgia Low-Speed Wind Tunnel (Continuation 1)

e.

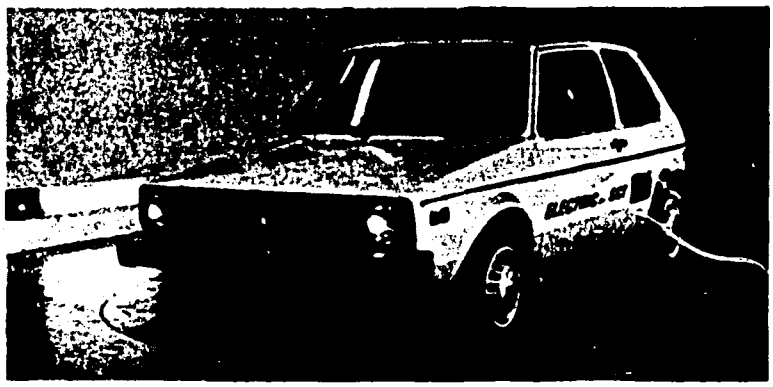

SCT Rabbit

C_{D_o}	A, m^2	$C_{D_o}A$, m^2
0.459	1.821	0.836

f.

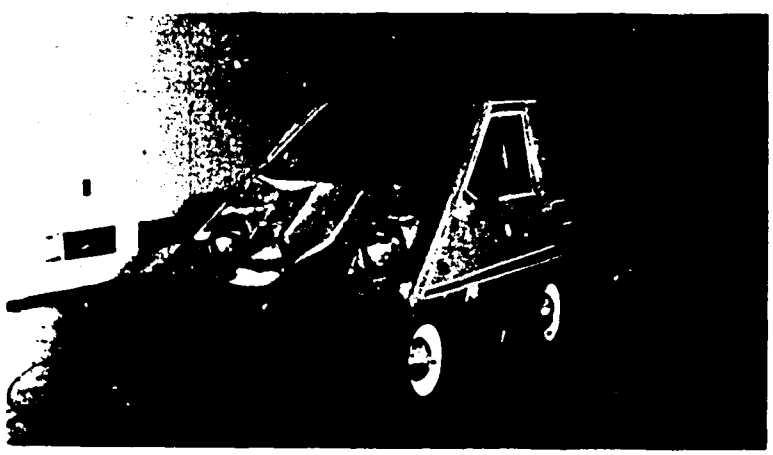

Sebring-Vanguard Citicar

C_{D_o}	A, m^2	$C_{D_o}A$, m^2
0.541	1.700	0.920

Figure B-3. Vehicles Tested in the Lockheed-Georgia Low-Speed Wind Tunnel (Continuation 2)

ORIGINAL PAGE IS
OF POOR QUALITY

g.

Zagato Elcar

C_{D_o}	A, m^2	$C_{D_o}A$, m^2
0.490	1.838	0.901

h.

Jet 600 Van

C_{D_o}	A, m^2	$C_{D_o}A$, m^2
0.539	1.942	1.029

Figure B-3. Vehicles Tested in the Lockheed-Georgia Low-Speed Wind Tunnel (Continuation 3)

ORIGINAL PAGE IS
OF POOR QUALITY

i.

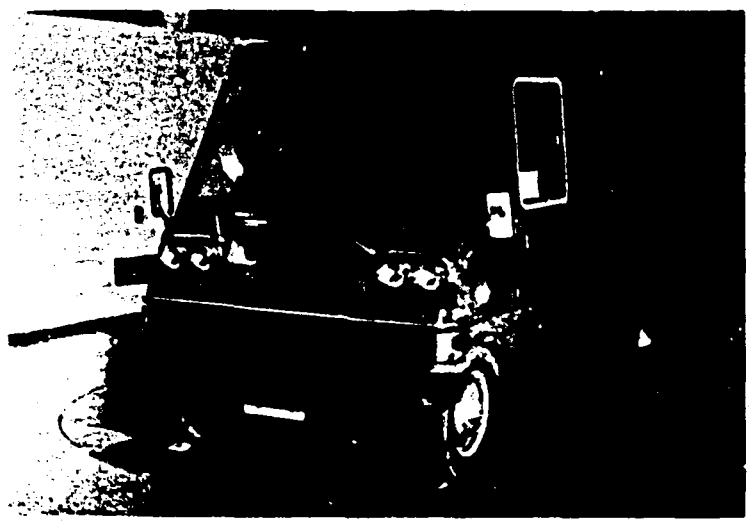

Otis Van

C_{D_o}	A, m^2	$C_{D_o}A$, m^2
0.581	2.593	1.507

j.

Kaylor GT

C_{D_o}	A, m^2	$C_{D_o}A$, m^2
0.583	1.359	0.792

Figure B-3. Vehicles Tested in the Lockheed-Georgia Low-Speed Wind Tunnel (Continuation 4)

k.

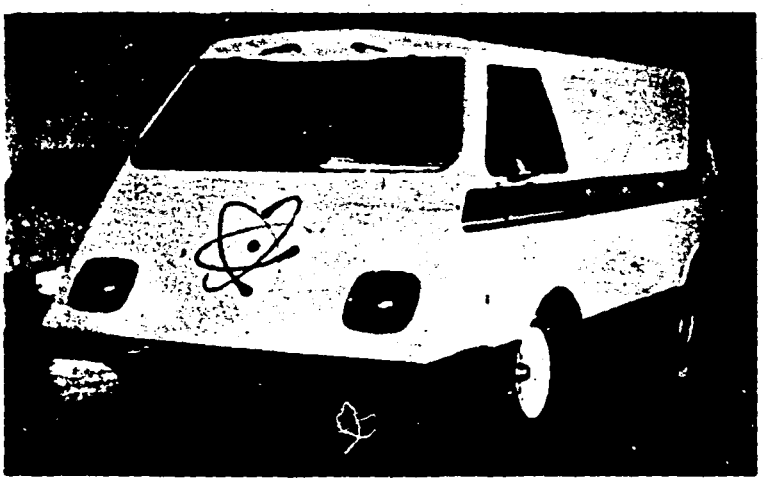

Energy R&D HEVAN

C_{D_o}	A, m^2	$C_{D_o}A$, m^2
0.497	3.283	1.632

l.

AMC Pacer Wagon

C_{D_o}	A, m^2	$C_{D_o}A$, m^2
0.406	2.225	0.903

Figure B-3. Vehicles Tested in the Lockheed-Georgia Low-Speed Wind Tunnel (Continuation 5)

m.

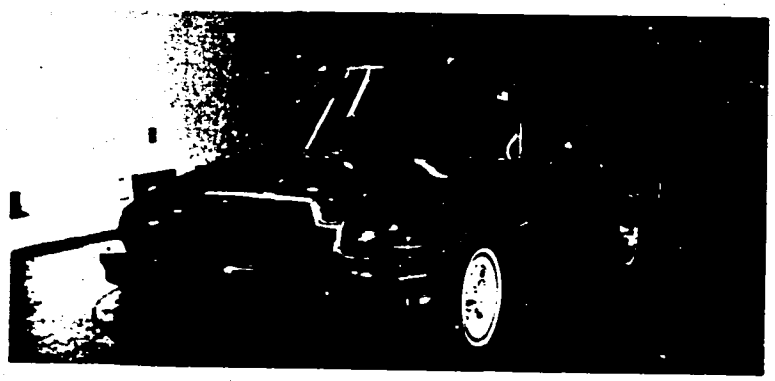

AMC Pacer Sedan

C_{D_o}	A, m^2	$C_{D_o}A$, m^2
0.450	2.222	1.000

n.

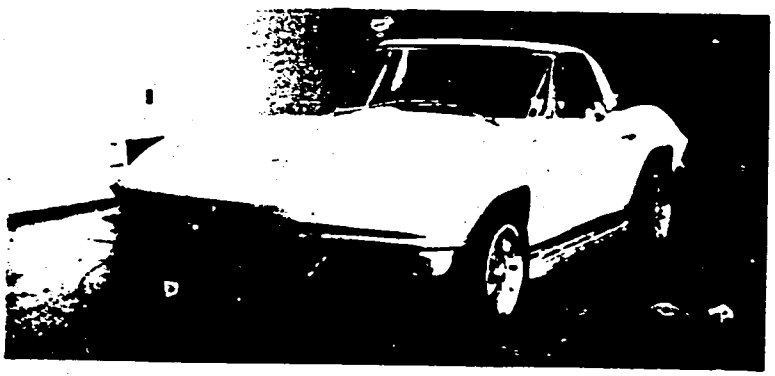

Chevrolet Corvette

C_{D_o}	A, m^2	$C_{D_o}A$, m^2
0.490	1.925	0.943

Figure B-3. Vehicles Tested in the Lockheed-Georgia Low-Speed Wind Tunnel (Continuation 6)

o.

Oldsmobile Delta 88 Sedan

C_{D_o}	A, m^2	$C_{D_o}A$, m^2
0.558	2.077	1.159

p.

Chevrolet Chevette

C_{D_o}	A, m^2	$C_{D_o}A$, m^2
0.502	1.765	0.886

Figure B-3. Vehicles Tested in the Lockheed-Georgia Low-Speed Wind Tunnel (Continuation 7)

q.

C_{D_o}	A, m^2	$C_{D_o}A$, m^2
0.411	1.906	0.783

r.

Honda Civic Sedan

C_{D_o}	A, m^2	$C_{D_o}A$, m^2
0.503	1.630	0.820

Figure B-1. Vehicles Tested in the Lockheed-Georgia Low-Speed Wind Tunnel (Continuation 8)

ORIGINAL PAGE IS
OF POOR QUALITY

s.

Honda Civic Wagon

C_{D_o}	A, m^2	$C_{D_o}A$, m^2
0.514	1.685	0.866

t.

Ford Fiesta

C_{D_o}	A, m^2	$C_{D_o}A$, m^2
0.468	1.747	0.818

Figure B-3. Vehicles Tested in the Lockheed-Georgia Low-Speed Wind Tunnel (Continuation 9)

APPENDIX C

A REVIEW OF GENERAL AERODYNAMIC DRAG PREDICTION PROCEDURES, APPLICATION, AND UTILITY

A. DRAG ESTIMATION METHODS

Several aerodynamicists have attempted to make generalizations or to predict a vehicle's drag based on various shape characteristics (References 3-1, 3-2, and C-1). The usual method is to assemble a large data base and develop correlations. Perhaps the best known effort is that of R.G.S. White (Reference 3-1) of Britain's Motor Industry Research Association (MIRA). Wind tunnel tests of 141 different vehicles were utilized. Each vehicle was divided into six basic zones, three of which were further subdivided. Numbers were assigned to features in each zone or subzone in an attempt to rate their obstructive effects on the airflow around the vehicle.

Rating values were assigned to each of the nine categories depending upon the vehicle's shape in those zones. The predicted drag coefficient was then determined from the following empirical equation:

$$C_D = 0.16 + 0.0095 \times \text{Drag Rating}$$

where the Drag Rating is simply the summation of the nine individual category ratings.

By way of verification, drag estimates for 20 vehicles (mainly European) were made by White using this procedure, and were then compared to measured values. The average scatter was about 7%. It should be pointed out that the drag of these vehicles was not particularly low, and that White's procedure would not necessarily reflect the subtleties inherent in drag-optimized vehicles. Another cautionary note is that measured MIRA drag values are substantially lower than similar measurements made in domestic wind tunnels. The real value of this effort is the relative ordering of the aerodynamic design consequences of several shape parameters.

A second, and less rigorous "drag rating" approach to drag estimates is presented in Reference C-1 (Cornish). Ten regions are defined and a rating of from 1 to 3 is assigned. On this basis, the most streamlined vehicle would have a rating (R) of 30 and the worst, a rating of 10. The resulting drag coefficient is then calculated from

$$C_D = 0.62 - 0.01R$$

This procedure is rather crude but simple and its accuracy is far less than the 7% reported for White's method.

PRECEDING PAGE BLANK NOT FILMED

Both of the two previous procedures are based upon shape correlation curves which are linear with the drag rating and are limited to conventional passenger vehicle configurations. A third estimation procedure, developed for the EPA (Pershing - Reference 3-2), is a "drag buildup" method based on quantitative geometric characteristics applicable to a large range of generic body shapes. The total vehicle drag coefficient is defined as the sum of the coefficients of 11 discrete parts.

$$C_{D_{tot}} = \sum_{i=1}^{11} C_{D_i}$$

Although this procedure requires more quantitative knowledge of the body shape being evaluated, it has the potential of addressing the more subtle details.

Excerpts from these three references follow; sufficient detail is included to allow their application. In addition, some generalizations are set forth concerning the drag increments characteristic of various components and devices.

B. DRAG ESTIMATION PROCEDURES

1. Drag Coefficient Estimation (R.G.S. White - Reference 3-1)

White divides a vehicle into six zones and three subzones for a total of nine categories. These are listed in Table C-1. A rating number is then assigned to the particular vehicle characteristic in each of the nine categories (see Table C-2). These nine intermediate ratings are summed to yield the "drag rating." The resulting drag coefficient is calculated from

$$C_D = 0.16 + (0.0095)\ (\text{Drag Rating})$$

Table C-1. Basic Vehicle Zones (Reference 3-1)

Zone	Subzone	Category
Front	(a) Outline plan	1
	(b) Elevation	2
Windshield/Roof Junction	(a) Cowl and fender cross section	3
	(b) Windshield plan	4
Roof	(a) Windshield peak	5
	(b) Roof plan	6
Rear Roof/Trunk		7
Lower Rear-End		8
Underbody		9

Table C-2. Drag Rating System[1]

Category 1. Front End Plan Outline		Rating
Approximately semicircular		1
Well-rounded outer quarters		2
Rounded corners without protuberances		3
Rounded corners with protuberances (a)		4
Squared tapering-in corners		5
Squared constant-width front		6

Category 2. Elevation(b)		Rating
Low rounded front, sloping up		1
High tapered rounded hood		
Low squared front, sloping up		2
High tapered squared hood		
Medium height rounded front, sloping up		3
Medium height squared front, sloping up		4
High rounded front, with horizontal hood	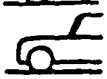	
High squared front, with horizontal hood	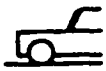	5

[1]Adapted from Reference 3-1.

Table C-2. Drag Rating System (Continuation 1)

Category 3. Cowl and Fender Cross-Section -Windshield/Roof Junction		Rating
Flush hood and fenders, well-rounded body sides		1
High cowl, low fenders		2
Hood flush with rounded-top fenders		3
High cowl, with rounded-top fenders		
Hood flush with squared-edged fenders		4
Depressed hood, with high squared-edged fenders		5
Category 4. Windshield Plant[c]		**Rating**
Full-wrap-around (approximately semicircular)		1
Wrapped-around ends	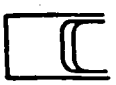	2
Bowed		3
Flat		4
Category 5. Windshield Peak		**Rating**
Rounded	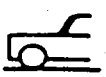	1
Squared (including flanges or gutters)	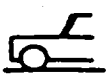	2
Forward-projecting peak		3

Table C-2. Drag Rating System (Continuation 2)

Category 6. Roof Plan		Rating
Well- or medium-tapered to rear	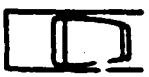	1
Tapering to front and rear (max. width at BC post) or approximately constant width		2
Tapering to front (max. width at rear)		3

Category 7. Rear Roof/Trunk(d)		Rating
Fastback (roof line continuous to tail)		1
Semi-fastback (with discontinuity in line to tail)		2
Squared roof with trunk rear edge squared	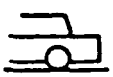	3
Rounded roof with rounded trunk		4
Squared roof with short or no trunk		
Rounded roof with short or no trunk		5

Table C-2. Drag Rating System (Continuation 3)

Category 8. Lower Rear End		Rating
Well- or medium-tapered to rear		1
Small taper to rear or constant width		2
Outward taper (or flared-out fins)		3

Category 9. Underbody(e)	Rating
Integral, flush floor, little projecting mechanism	1
Intermediate	2
Integral, projecting structure	3
Intermediate	4
Deep chassis	5

(a) Fender mirrors. Include in protuberances if at the fender leading end. Otherwise add 1.

(b) Add: 3 for separate fenders; 4 for open front to fenders (above bumper level); 2 for raised built-in headlamps; 4 for small separate headlamps; 7 for large separate headlamps.

(c) Add: 1 for upright windshield; 1 for prominent flanges or rain gutters.

(d) Add: 3 for high fins or sharp longitudinal edges to trunk; 2 for separate fenders. Note: In all the ratings in this column, the trunk is assumed to be rounded laterally.

(e) Intermediate ratings applied from vehicle examination.

NOTE: Throughout table, the word "taper" or "tapered" refers to the plan view.

2. Drag Coefficient Estimation (J. J. Cornish - Reference C-1)

Cornish divides a vehicle into 10 zones and assigns a sub-rating of from 1 to 3 to each of them (see Table C-3). The total rating, R, is the sum of these 10 sub-ratings. Two windshield zone items (numbers 4 and 5) refer to the elevation and plan views, respectively. The resulting drag coefficient is calculated from

$$C_D = 0.62 - 0.01R$$

Table C-3. Aerodynamic Rating

No.	Item	1	2	3
1	Grill	Blunt; square	Fairly sloped	Well sloped
2	Lights	Open; exposed	Partially inset	Well faired
3	Hood	Flat	Fairly sloped	Convex, sloped
4	Windshield	Steep	Fairly sloped	Well sloped
5	Windshield	Flat	Fairly curved	Well curved
6	Roof top	Open	Fairly sloped	Convex, sloped
7	Rear Window	Notched	Fairly sloped	Fastback type
8	Trunk	Cut off square	Fairly sloped	Fastback type
9	Wheels	Exposed	Partially closed	Well concealed
10	Underside	Exposed	Partial pan	Full pan

3. Drag Coefficient Estimation (B. Pershing - Reference 3-2)

This procedure is much more complicated but much less subjective than the previous two. The relevant vehicle dimensions and areas are illustrated in Figures C-1 and C-2. The total drag coefficient is defined as the summation of eleven component coefficients:

$$C_{D_{tot}} = \sum_{i=1}^{11} C_{D_i}$$

The details of the determination of the ith components follow (reproduced directly from Reference 3-2). An assessment of this procedure is given in Reference 3-3.

Front End Drag Coefficient, C_{D_1}

$$C_{D_1} = 0.707 \left(\frac{A_F}{A_R}\right) \left\{1.0 - 2.79 \left(\frac{R}{E}\right)_u + 0.82 \left(\frac{R}{E}\right)_l - 5.21 \left(\frac{R}{E}\right)_v - 29.5 \left(\frac{R}{E}\right)_u \left(\frac{R}{E}\right)_l \left[1.0 - 2.25 \left(\frac{R}{E}\right)_v\right]\right\}$$

where

A_R = total vehicle projected frontal area, m^2 (ft^2)
A_F = front end projected area, m^2 (ft^2)
R = edge radius, m (ft)
E = running length of the edge radius, m (ft)

and the subscripts u, l, and v refer to the upper, lower, and vertical edges of the front end, respectively. The $(R/E)_i$ are to be taken as 0.105 when the estimated values exceed this magnitude.

Windshield Drag Coefficient, C_{D_2}

$$C_{D_2} = 0.707 \left(\frac{A_W}{A_R}\right)\left[1.0 - 2.79 \left(\frac{R}{E}\right)_{u'} \cos\beta - 5.21 \left(\frac{R}{E}\right)_{v'}\right] \cos^2\gamma$$

where

A_W = projected area of windshield, m^2 (ft^2)
γ = slope of the windshield measured from the vertical, deg
$\beta = 2\gamma$

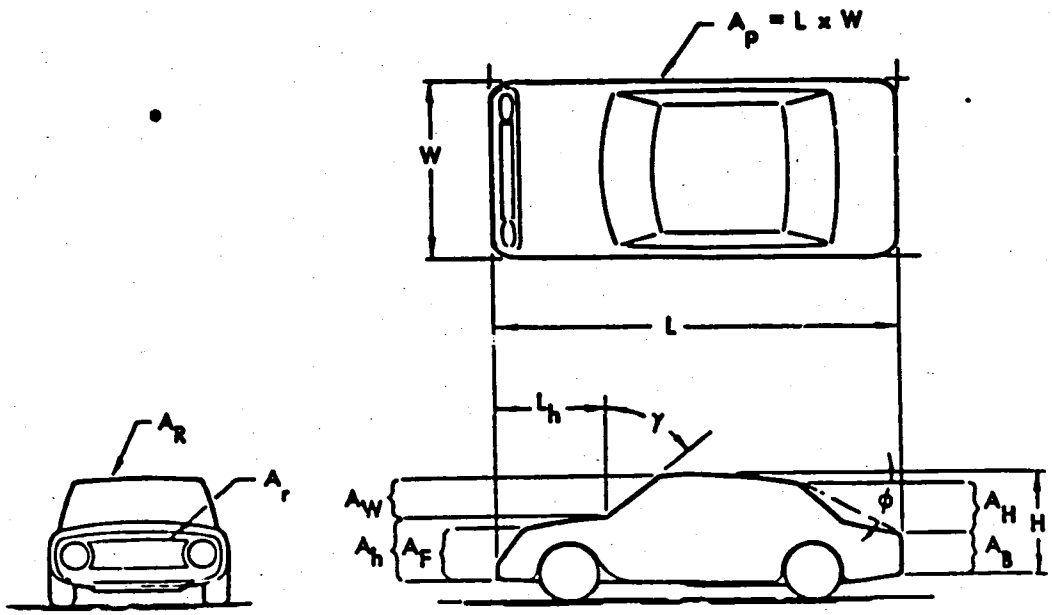

Figure C-1. Vehicle Dimensions (Reference 3-2)

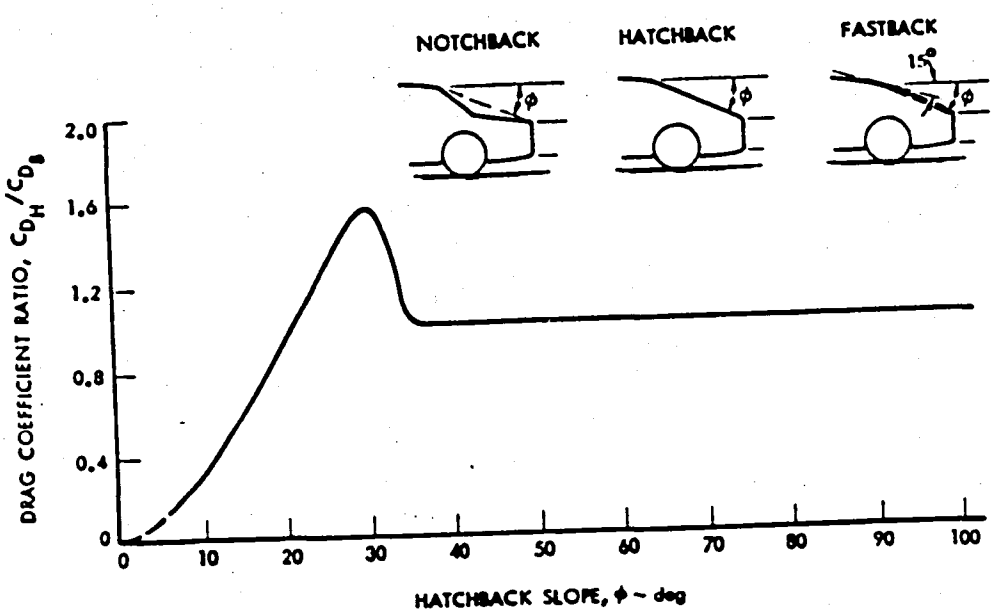

Figure C-2. Hatchback-Notchback Drag Coefficient Ratio

and the subscripts u' and v' refer to the roof-windshield intersection and the windshield posts, respectively. The value of $\cos\gamma$ is to be taken as zero for γ larger than 45 degrees and the $(R/E)_i$ are to be taken as 0.105 for estimated values exceeding this magnitude.

Front Hood Drag Coefficient, C_{D_3}

$$C_{D_3} = 0.707\left(\frac{A_h - A_F}{L_h}\right)^2 \Big/ A_R$$

where

A_h = projected area of body below the hood-windshield intersection, m^2 (ft^2)
L_h = length of hood in the elevation or side view, m (ft) and the quantity $(A_h - A_F)$ is to be taken as zero if it is negative.

Rear Vertical Edge Drag Coefficient, C_{D_4}

$$C_{D_4} = -0.19\left(\frac{R_v}{W}\right)\left(\frac{E_b}{H}\right) \quad \text{for } \left(\frac{R_v}{W}\right) \leq 0.105$$

$$= -0.02\left(\frac{E_b}{H}\right) \quad \text{for } \left(\frac{R_v}{W}\right) > 0.105$$

where

R_v = radius of rear vertical edges, m (ft)
W = vehicle width, m (ft)
E_b = length of rear vertical edge radius, m (ft)
H = vehicle height, m (ft)

Base Region Drag Coefficient, C_{D_5}

$$C_{D_5} = 0.15\left[\left(\frac{A_B}{A_R}\right) + \left(\frac{C_{D_H}}{C_{D_B}}\right)\left(\frac{A_H}{A_R}\right)\right]$$

where

A_B = projected area of flat portion of base region
A_H = projected area of upper rear or hatch portion of base region measured from the upper rear roof break (or for smoothly curved rooflines, that point where the roofline slope is 15 degrees) to the top of the flat base, m^2 (ft^2)
C_{D_B} = drag coefficient of the flat base

C_{D_H} = drag coefficient of the upper rear or hatch portion of the base region

and the ratio (C_D/C_{D_B}) is shown in Figure C-2 as a function of ϕ, the angle of the line from the upper rear roof break to the top of the flat base as measured from the horizontal.

Underbody Drag Coefficient, C_{D_6}

$$C_{D_6} = 0.025\ (0.5 - x/L) \left(\frac{A_P}{A_R}\right) \quad \text{for } 0 \leq x/L \leq 0.5$$

$$= 0 \quad \text{for } x/L > 0.5$$

where

x = smoothed forward length of the underbody, m (ft)
L = vehicle length, m (ft)
A_P = projected plan area of the vehicle, m^2 (ft^2)

Wheel and Wheel Well Drag Coefficient, C_{D_7}

$$C_{D_7} = 0.14$$

Rear Wheel Well Fairing Drag Coefficient, C_{D_8}

$$C_{D_8} = -0.01$$

Protuberance Drag Coefficient, C_{D_9}

$$C_{D_9} = \frac{1.1}{A_R} \sum A_{P_j}$$

where

A_{P_j} = projected area of jth protuberance, m^2 (ft^2)

Bullet Mirror Drag Coefficient, $C_{D_{10}}$

$$C_{D_{10}} = 0.4\ \frac{A_M}{A_R}$$

where

A_M = projected area of mirror with bullet fairing, m^2 (ft^2)

Cooling Drag Coefficient, $C_{D_{11}}$

$$C_{D_{11}} = 1.8\left(\frac{A_r}{A_R}\right)\left(\frac{u_r}{u}\right)\left[1.0 - 0.75\left(\frac{u_r}{u}\right)\right]$$

where

A_r = radiator area, m^2 (ft^2)
u_r = exit velocity of cooling air from radiator
(u_r/u) = $0.233\ [1.0 - k\ (u/100)^2]$

and

k = $1.140\ (m/sec)^{-2}$ $\left[\text{or } 0.299\ (mph)^{-2}\right]$

4. Drag Increment Generalizations

General rule-of-thumb values have been given to many interference components and drag reduction devices. These are helpful only in the broadest sense; that is, most effects are a function of the specific application. For instance, a front air dam (or chin spoiler) might significantly reduce the drag for one vehicle but increase it for another. Similarly, some low-drag device may be detrimental at a yaw angle. Such dramatic results, however, are generally reserved for special cases. If one limits the application to an "average, conventional sedan," perhaps the generalizations in Table C-4 can provide some guidelines. The increments should not be considered as purely additive; this is particularly obvious in the case of an underpan and air dam.

Table C-4. Drag Increment Generalizations

Component or Configuration	C_{D_o} (%)	Reference(s)
Full length underpan	-5 to -15	3-8, 3-10, C-2, C-3
Front "chin" spoiler (air dam)	-6 to -9	3-8, 3-9, C-4
Rear deck spoiled (lip)	-5 to -9	3-8, 3-9, C-3, C-4
Flush windshield and side glass (no raingutters)	-3 to -7	3-10, C-5
Wheel discs and rear fender skirts	0 to -2	3-10, C-4
Sideview mirror(s)		
Conventional A - pillar, stalk mount	+1 to +4	3-10, B-4, C-5
A - pillar, integral mount	+1 to +2	3-10
Fender mount (two)	+6	3-10
Headlights		
Pop-up	+3 to +6	3-10, C-6
Pocket	+3 to +6	3-10
Open front windows	0 to +3	3-8, C-2, C-6
Body side rubstrip	+1	3-10
Road trim package[1]	+2 to +8	3-10, B-4,

[1] Consists of conventional mirror, windshield wipers, door handles, license plate, body gaps.

APPENDIX D

APPLICATION OF AREA-DISTRIBUTION SMOOTHING PROCEDURES TO AUTOMOTIVE AERODYNAMIC DESIGN

Basic Principles

Since early times, man has recognized that certain shapes found in nature move more efficiently through air and water. The hulls of even primitive ships were often modeled after the well-known tear drop-shaped body exhibited by many fish and birds. It was therefore only logical that early attempts to streamline automotive shapes were approached in a similar manner. These often took the form of a "torpedo on wheels" or the superposition of several "half drop" shapes. However, these potentially low drag designs were often severely compromised by many unfaired appendages such as wheels, lights, suspension members, open cockpits and the like.

The basic principle demonstrated by low drag bodies found in nature, however, can still find application in road vehicles. A "streamlined" body has low drag by virtue of well attached flow (no boundary layer separation) and the resultant minimum size wake. This boundary layer (flow immediately adjacent to the body surface), will remain attached as the flow negotiates its way along a smooth body so long as its momentum is sufficient to overcome any adverse pressure gradient. Momentum loss, however, is a function of the body surface contour gradients in the direction of flow. A well streamlined body has only moderate contour gradients whereas a modern automobile is characterized by many steep gradients. A representative contour parameter suggested by Hucho in Reference 3-4 is the line integral of the rate of change of curvature along the body surface. For simplicity, Hucho considers only the integral along the body centerline but it is recognized, that it should be applied over the entire body surface. Although theoretically possible, this would require a tremendous effort.

The present principle suggests a simple, if imperfect, compromise. The distribution of cross-sectional area as a function of longitudinal station along the body may be an approximation, representative of an integrated body contour parameter. The area distribution principle may be stated thusly:

> "Gradual area variations along a body length are characteristic of a streamlined design."

It is pointed out that this may be a necessary, if not sufficient, attribute. Clearly, one could conceive of a shape satisfying the smooth area distribution criteria with cavities opposite sharp lumps and bumps canceling their effect. In order to minimize that particular anomaly, a corollary is added to the principle:

> "The body camber-line should be as smooth as possible."

PRECEDING PAGE BLANK NOT FILMED

Here the camber-line is defined as the locus of points connecting the centroids of the cross-sectional area slices. Although the emphasis is different[1] these simplified principles are in general agreement with Reference 3-5.

Procedure

The application of the area distribution and camber-line principles represents an attempt to provide an intermediate alternative to costly developmental wind tunnel testing. Although the procedure relies heavily on perceptive decisions, it does produce an analytical/graphical evaluation process which iteratively guides one to a more streamlined design.

Before the process can be implemented it is necessary to have rather detailed three-view loft drawings or station templates of the candidate body. Section views may then be created at about 5 to 10 cm intervals (full-scale) along the longitudinal axis (more frequently where the area is perceived to be changing rapidly and fewer where the area change is less dramatic). A planimeter (or other means) may then be used to measure the area of each cross section. The areas, thus determined, are then plotted as a function of station position. Figure D-1 is a schematic example of the procedure and the result. The diagram created in this manner is called the body "area distribution." Those regions where the area is changing rapidly are candidates for modification. However, in order to help guide these modifications, the corresponding body camber-line should be developed. As indicated earlier, this is merely a plot of the section area centroids versus station position. An easy way of determining the centroid of a section area is to first cut the shape out of a piece of stiff paper or cardboard. Next, suspend it from a pin near the perimeter at some arbitrary point (such that it's free to rotate) and draw a vertical line through the pin hole. Rotate the shape about 90° and repeat. If the material is homogeneous, the intersection of the two lines will be the centroid. Obviously, the point should lie midway between the sides of each section or the design is not laterally symmetrical. The vertical displacement from some reference such as the ground varies from section to section. These measurements when plotted versus section position, produce the body camber-line. (This result is also depicted in Figure D-1.) With the added constraint that the camber-line be as smooth as possible, the sections requiring area modifications are reexamined. If it appears that some area needs to be added at a few stations (in order to smooth the hood/windshield interface, for example) and the camber-line is low in that region, then the area should be added near the upper surfaces. If the camber-line could be smoothed by lowering it in that region,

---

[1]Morelli, in developing his "Body Shape of Minimum Drag" (Reference 3-5), begins by defining a specialized camber-line and bases the body shape upon it.

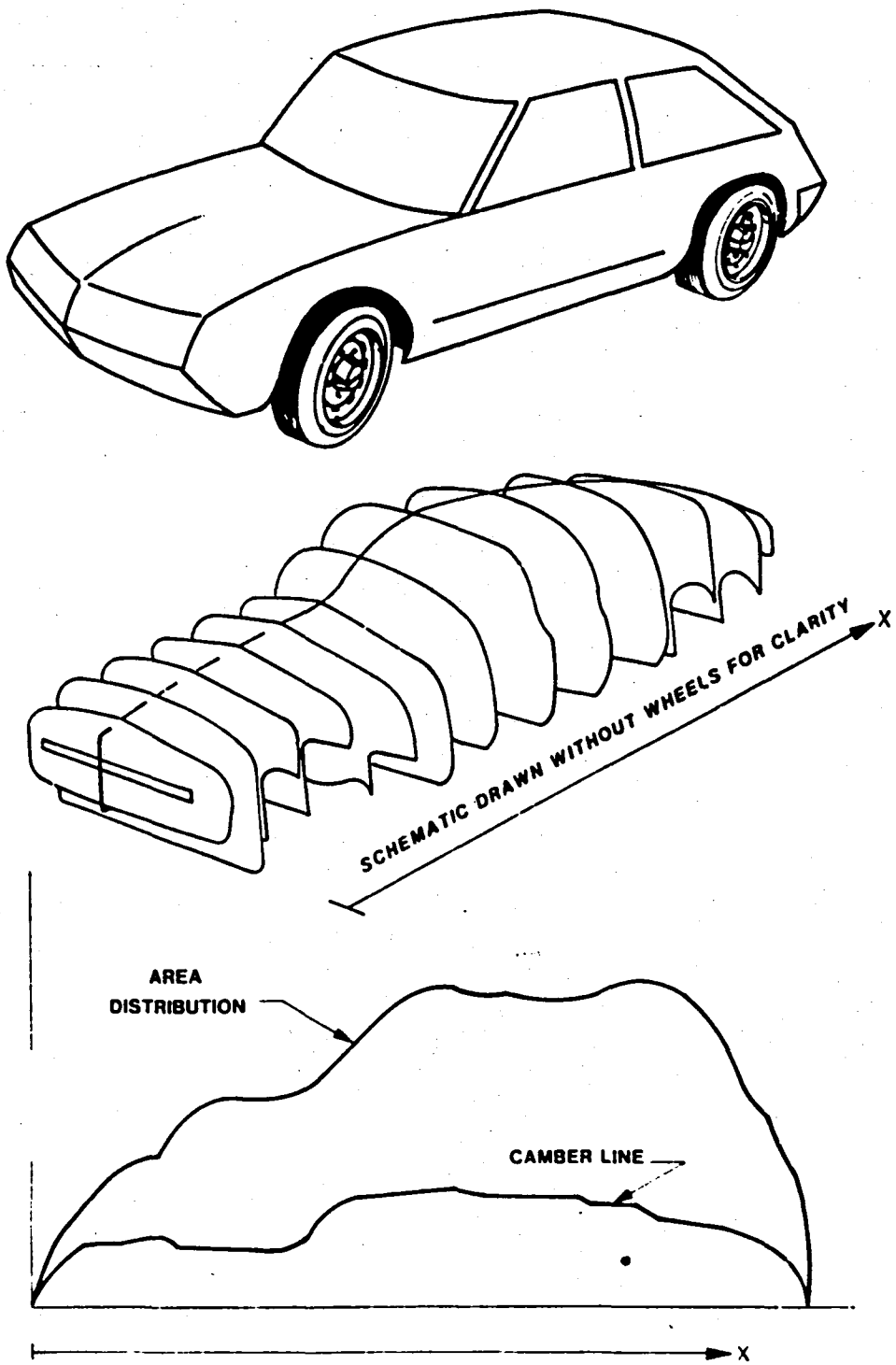

Figure D-1. Schematic Showing Area Distribution Procedure

the area should be added below the centroid. It is generally advisable to make this area addition around the rocker panel rather than under the body. The technique is iterative, and the area distribution and camber-line curves should be checked following each complete modification. Quite clearly, this procedure cannot be mindlessly applied, but rather requires a blend of artistic style and sensible judgement. Certain individuals may be able to accomplish much the same result by "integrating with their eye" but in any event, this technique provides a methodology to measure the designer's intuition.

Examples

The General Electric ETV-1 represents an exceptionally well integrated low-drag (C_{D_o} = 0.3) vehicle body (Figure D-2a). It was designed by Chrysler using subscale developmental wind tunnel test techniques on a series of clay models (Reference B-5). Nevertheless, it is interesting to examine its area distribution in order to test the area distribution principle. That is, does this low-drag vehicle exhibit the gradual area variation typical of naturally streamlined bodies? Figure D-2b shows that the ETV-1 area distribution is fairly smooth. However, without some basis for comparison it is difficult to assess whether a particular area curve is exceptional or whether there is room for improvement. An example of a low drag design, near the extreme practical limit for an automotive shape, was developed using the area distribution technique described earlier and verified in subsequent wind tunnel tests (Figure D-3a).[1] The styling theme is clearly reminiscent of the "Body Shape of Minimum Drag" developed by Morelli (Reference 3-5). The area distribution resulting from this very streamlined, low-drag design is shown in Figure D-3b. Obviously, the gradient is smooth since the design was refined using that technique. Both the ETV-1 and this design (Mays-B) are drag-optimized shapes for their respective design themes. It should be pointed out, however, that the former was developed through costly wind tunnel developmental testing (equivalent to a Level III Design) and the latter using the area gradient principle (equivalent to a Level II Design).

A third example is the Garrett AiResearch ETV-2 electric vehicle (Figure D-4a) which employed neither of these processes during design. In fact, this vehicle is representative of a Level I Design. As shown in Figure D-4b, the area distribution of the Garrett vehicle

---

[1]This work was performed under subcontract to the Art Center College of Design in Pasadena as a student project by J.C. Mays (Reference D-1). This outstanding design was found to have a C_{D_o} = 0.2 from clay model wind tunnel tests. Further alterations in the tunnel paid no drag dividends; it had indeed been drag optimized on paper. (Since the model lacked a certain level of detail, which would be present on an actual vehicle, it is estimated that a prototype version might have a drag coefficient around 0.25.)

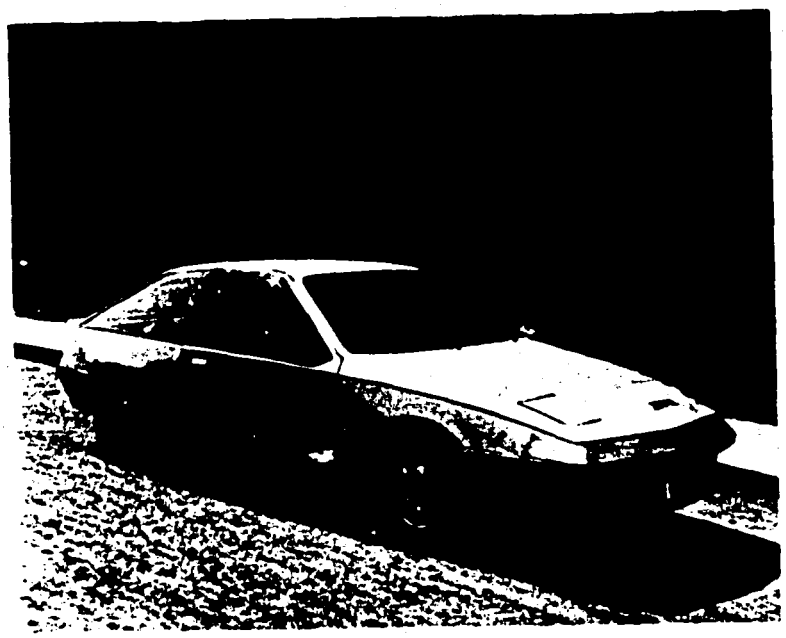

Figure D-2a. General Electric ETV-1

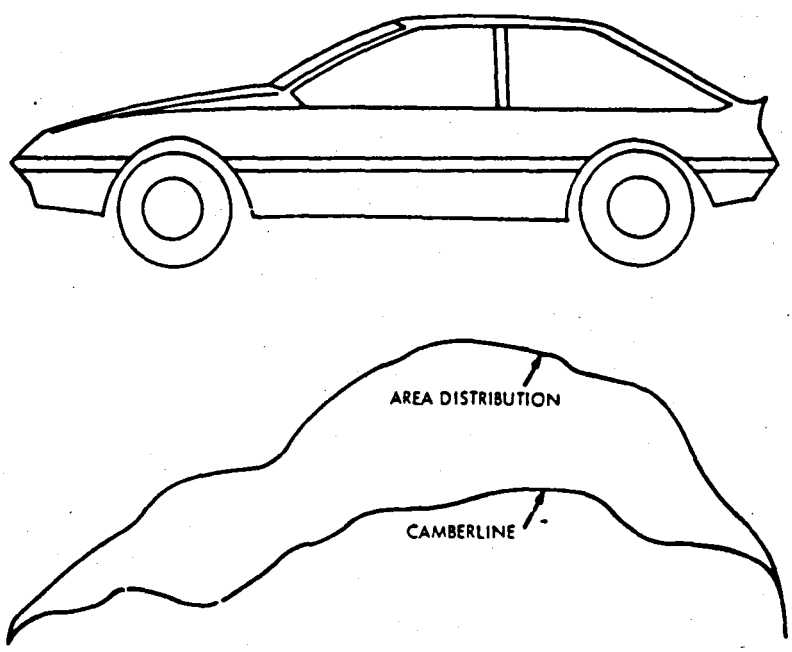

Figure D-2b. Area Distribution and Camber-Line for the General Electric ETV-1

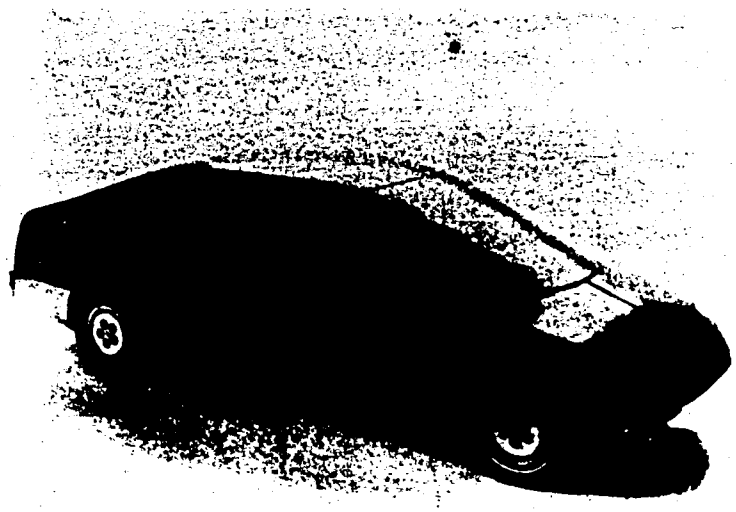

Figure D-3a. Mays Aero Car (Model)

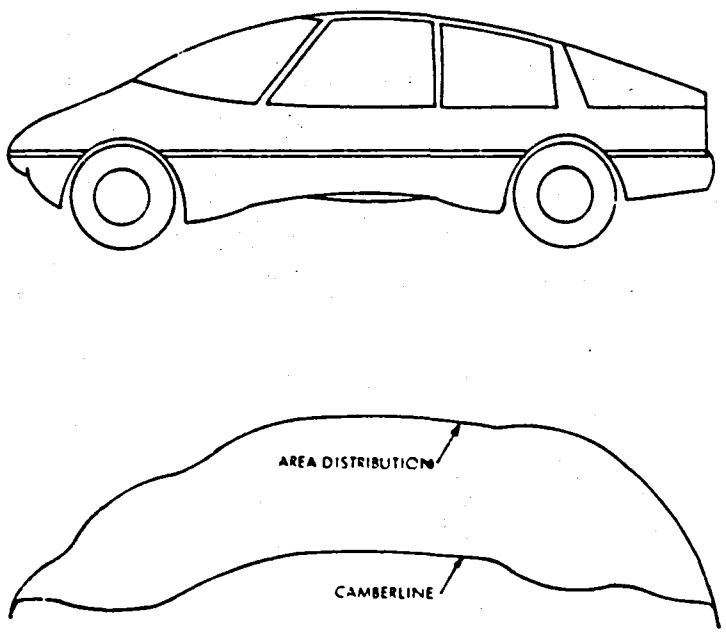

Figure D-3b. Area Distribution and Camber-Line for the Mays Aero Car

Figure D-4a. Garrett AiResearch ETV-2

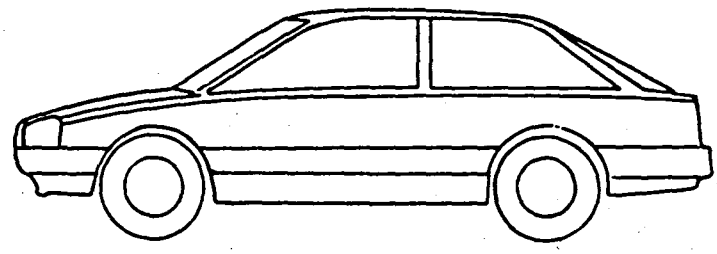

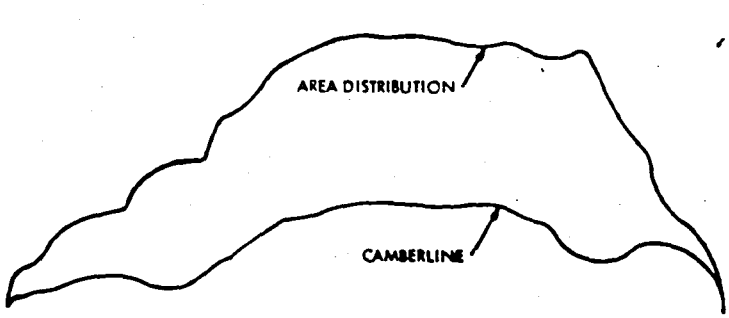

Figure D-4b. Area Distribution and Camber-Line for the Garrett AiResearch ETV-2

is significantly rougher than either of the other two vehicle shapes. This is consistent with full-scale wind tunnel test results which found the Garrett drag coefficient to be about 0.4 (significantly greater than either of the other two example vehicles).

These few examples by no means provide conclusive proof of the area distribution principle but there is sufficient evidence of its value to include it as a part of the design strategy.

APPENDIX E

ESTIMATING DRAG CHARACTERISTICS IN YAW FOR AUTOMOBILE SHAPES

Since a road vehicle operates in the presence of ambient winds which are rarely aligned with its longitudinal axis, some knowledge of the relationship between drag and yaw angle is necessary. The first and most significant effort to quantify and generalize these characteristics for automotive shapes was performed by Barth of the Stuttgart Technical College (Reference E-1) two decades ago. Limited to side force and yawing moment coefficients, his results were derived from wind tunnel tests of four basic shapes and four groups of small automobile models totaling 28 specimens in all. He showed that variations with yaw angle were generally linear (up to 25°) and that differences in body form and features affected only the slope of the variation. The body features upon which Barth based his correlations were aspect ratio and fineness ratio.

Ten years later, recognizing the need to generalize yaw effects for all the aerodynamic coefficients (particularly drag), Bowman of Ford Motor Company compiled wind tunnel data on 3/8-scale models of 21 automobile body forms (Reference 3-6). Suggesting that the range of aspect ratios for prevailing American sedans was not sufficiently large enough to provide a suitable correlation parameter, he looked for non-geometric relationships. Specifically, he determined that the drag-yaw characteristic had a typical maximum of about 30° and the amplitude was a function of the drag coefficient at zero yaw. Bowman's general equation was of the form:

$$C_D = C_{D_o} + K_1(1 - \cos 6\psi) \qquad \text{(E-1)}$$

where K_1 is a function of C_{D_o} (the zero-yaw drag coefficient) and a few general shape descriptions; ψ is the yaw angle in degrees.

In an effort to correlate the model and full-scale wind tunnel data developed during the present program, it was determined that Bowman's representation was entirely inadequate to represent the range of vehicles investigated. Since extensive model tests had been performed on the effects of aspect and fineness ratios for automotive shapes (see Appendix A), these data were examined for yaw characteristic correlations. Using a formulation format similar to Bowman's, the following equation was derived:

$$C_D/C_{D_o} = 1 + K(1 - \cos 6\psi) \qquad \text{(E-2)}$$

where K is not a function of C_{D_o} but a function of aspect ratio (AR) and fineness ratio (FR). That is,

$$K = (0.15AR - 0.03)FR - 0.513AR + 0.336 \qquad \text{(E-3)}$$

where AR is the ratio of body height (not including ground clearance) to body width, and FR is the ratio of body length to the diameter of a circle equivalent to the body frontal area.

The fit to the experimental data is quite good, as is shown in the following table:

AR	FR	K measured	K Eq. E-3
0.58	2.2	0.16	0.16
	2.7	0.19	0.19
	3.2	0.22	0.22
0.70	2.2	0.13	0.14
	2.7	0.18	0.18
	3.2	0.22	0.22
0.77	2.2	0.14	0.13
	2.7	0.19	0.17
	3.2	0.22	0.21
0.88	2.2	0.10	0.11
	2.7	0.14	0.16
	3.2	0.16	0.21

Encouraged by this clear correlation, Equation E-3 was applied and compared to the results of the full scale prototype wind tunnel tests (Reference 2-1). Because the simple AR and FR parameters did not adequately describe the details of each vehicle shape, the correlation was not nearly as good. However, for design purposes, this equation should suffice for typical hatchback or fastback subcompact vehicles. A few modifying comments are necessary, however, for vehicles with specifically distinctive characteristics.

In summary, the variation of drag with yaw angle can, to a first approximation, be described by the following function and associated comments:

$$C_D/C_{D_o} = 1 + K(1 - \cos 6\psi) \qquad \text{(E-2)}$$

where

$$K = (0.15AR - 0.03)FR - 0.513AR + 0.336 \qquad \text{(E-3)}$$

- Not valid for fineness ratios less than 1.5.
- Reduce K by up to 50% for extremely low nose and sloping hoodlines.
- Increase K by up to 10% for harsh, angular design with corner radii less than 10 cm.
- Increase K by up to 15% for notch back designs.

Note that a maximum is reached at $\psi = 30^o$ such that,

$$C_{D_{max}}/C_{D_o} = 1 + 2K \qquad \text{(E-4)}$$

This parameter is useful in predicting the effects of ambient winds in Appendix F.

APPENDIX F

DETERMINATION OF DRAG WIND-WEIGHTING FACTORS FOR VEHICLES OPERATING IN AMBIENT WINDS

As a vehicle moves along a roadway, it normally operates in a windy environment. Since the wind vector is usually not aligned with the highway, the vehicle is effectively yawed with respect to the flow. Therefore, range predictions that utilize the zero-yaw drag values will inaccurately characterize the aerodynamic contribution and yield optimistic results.

A procedure to accurately determine the effects of ambient winds on vehicle drag has recently been developed (Reference 3-7). The approach is to figuratively (in a computer simulation) drive a vehicle over a prescribed velocity-time schedule in the presence of a wind which varies statistically in speed (a speed probability function designated by some annual mean wind speed) and comes with equal probability from any direction. The resultant combination of the vehicle and wind velocity vectors yields an instantaneous yaw angle with respect to the vehicle. If the vehicle's drag-yaw characteristic is known or assumed, the resultant drag may be determined at each instant. Therefore, the energy required to overcome aerodynamic resistance is calculated by integrating the instantaneous aerodynamic power required over the entire cycle. It is then possible to determine the <u>constant</u> drag coefficient that would have been necessary in order to yield the same result. The ratio of this new effective coefficient, $C_{D_{eff}}$, to the original zero-yaw drag coefficient, C_{D_o}, is the wind weighting factor, F. F is thus a multiplier to correct the zero-yaw drag coefficient for the effects of ambient winds.

This rigorous procedure was used to generate F-factors for a large range of vehicle characteristics, wind conditions, and driving cycles. Analysis of these results yielded many fortuitous relationships leading to simplifying assumptions which are accurate to within about 3%.

The wind-weighting factor, F, was found to be a simple exponential function of the dominant parameter, $C_{D_{max}}/C_{D_o}$; the yaw angle where $C_{D_{max}}$ occurs ($\psi = 30^o \pm 5^o$) is of second order significance and is neglected. For design purposes, the parameter $C_{D_{max}}/C_{D_o}$ may be estimated by a special case of the yaw characteristic equation presented in Appendix E (Equation E-4). F is then only a function of yaw angle, the annual mean wind speed and the particular driving cycle or constant speed. The resulting equations for F are given in Tables F-1 and F-2 in metric and English units, respectively.

Table F-1. Wind-Weighting Factor Equations - Metric Units

W = annual mean wind speed in km/hr (12 km/hr mean average in U.S.)
V = vehicle speed in km/hr

EPA CYCLES

URBAN:

$$F = (1.22 \times 10^{-4}W^2 + 1.61 \times 10^{-2}W) \times (C_{D_{max}}/C_{D_o}) + 2.89 \times 10^{-4}W^2 - 1.47 \times 10^{-2}W + 1.0$$

HIGHWAY:

$$F = (1.94 \times 10^{-4}W^2 + 5.61 \times 10^{-3}W) \times (C_{D_{max}}/C_{D_o}) + 2.86 \times 10^{-5}W^2 - 5.32 \times 10^{-3}W + 1.0$$

COMBINED: (55% - 45% split):

$$F = (1.72 \times 10^{-4}W^2 + 1.11 \times 10^{-2}W) \times (C_{D_{max}}/C_{D_o}) + 1.40 \times 10^{-4}W^2 - 1.11 \times 10^{-2}W + 1.0$$

SAE ELECTRIC CYCLES (J227a)

B: $$F = (9.41 \times 10^{-5}W^2 + 3.76 \times 10^{-2}W) \times (C_{D_{max}}/C_{D_o}) + 5.97 \times 10^{-4}W^2 - 2.83 \times 10^{-2}W + 1.0$$

C: $$F = (1.18 \times 10^{-4}W^2 + 2.22 \times 10^{-2}W) \times (C_{D_{max}}/ CD_o) + 3.61 \times 10^{-4}W^2 - 1.94 \times 10^{-2}W + 1.0$$

D: $$F = (1.81 \times 10^{-4}W^2 + 1.25 \times 10^{-2}W) \times (C_{D_{max}}/CD_o) + 1.44 \times 10^{-4}W^2 - 1.33 \times 10^{-2}W + 1.0$$

CONSTANT SPEED

$$F = \left[0.98\ (W/V)2 + 0.63\ (W/V)\right] \times (C_{D_{max}}/C_{D_o}) - 0.40\ (W/V) + 1.0$$

Constraints:[1]

For $(W/V) < 0.09$ $F = 1.0$
For $(W/V) > 1.0$ $(W/V) = 1.0$

[1]These constraints may be necessary if this equation is applied to the quasi-steady instantaneous vehicle speeds in a computer simulation (i.e., the function goes to infinity at V = 0). In a physical sense, however, the equation is entirely proper without these boundary conditions.

Table F-2. Wind-Weighting Factor Equation - English Units

W = annual mean wind speed in mph (7.5 mph mean average in U.S.)
V = vehicle speed in mph

EPA CYCLES

URBAN:

$$F = (3.16 \times 10^{-4}W^2 + 2.59 \times 10^{-2}W) \times (C_{D_{max}}/C_{D_o}) + 7.49 \times 10^{-4}W^2 - 2.37 \times 10^{-2}W + 1.0$$

HIGHWAY:

$$F = (5.02 \times 10^{-4}W^2 + 9.04 \times 10^{-3}W) \times (C_{D_{max}}/C_{D_o}) + 7.41 \times 10^{-5}W^2 - 8.56 \times 10^{-3}W + 1.0$$

COMBINED: (55% - 45% split):

$$B: F = (4.47 \times 10^{-4}W^2 + 1.78 \times 10^{-2}W) \times (C_{D_{max}}/C_{D_o}) + 3.62 \times 10^{-3}W^2 - 1.79 \times 10^{-2}W + 1.0$$

SAE ELECTRIC CYCLES (J227a)

$$B: F = (2.44 \times 10^{-4}W^2 + 6.06 \times 10^{-2}W) \times (C_{D_{max}}/C_{D_o}) + 1.55 \times 10^{-3}W^2 - 4.56 \times 10^{-2}W + 1.0$$

$$C: F = (3.07 \times 10^{-4}W^2 + 3.57 \times 10^{-2}W) \times (C_{D_{max}}/C_{D_o}) + 9.37 \times 10^{-4}W^2 - 3.12 \times 10^{-2}W + 1.0$$

$$D: F = (4.68 \times 10^{-4}W^2 + 2.01 \times 10^{-2}W) \times (C_{D_{max}}/C_{D_o}) + 3.73 \times 10^{-4}W^2 - 2.14 \times 10^{-2}W + 1.0$$

CONSTANT SPEED

$$F = \left[0.98(W/V)^2 + 0.63(W/V)\right] \times (C_{D_{max}}/C_{D_o}) - 0.40(W/V) + 1.0$$

Constraints:

For $(W/V) < 0.09$ $F = 1.0$
For $(W/V) > 1.0$ $(W/V) = 1.0$

In order to further simplify the application, Figures F-1 and F-2 are is presented. These are graphical representations from Table F-1 with the annual mean wind speed fixed at 12 km/hr (7.5 mph);[1] this is the average condition across the country.

Therefore, in the course of the design process, after the zero-yaw drag coefficient, C_{D_o}, has been estimated, the effective wind weighted coefficient $C_{D_{eff}}$ may be determined by

(1) Calculating the $C_{D_{max}}/C_{D_o}$ ratio from Equation E-4.

(2) Determining F, for the design cycle, from Figure F-1 or F-2.

(3) Calculating, $C_{D_{eff}} = F \times C_{D_o}$.

An example to demonstrate just how important the wind weighting analysis might be in making drag estimations is presented in Table F-3. Using the vehicles in the EHV Aerodynamic Data Base (Appendix B, Part C), the effective wind weighted drag coefficient, $C_{D_{eff}}$, was determined (for operation over a J227a D cycle). In this case the $C_{D_{max}}/C_{D_o}$ ratio was precisely known for each vehicle from wind tunnel test data at yaw angles up to 40°. Therefore, the wind weighting factor, F, could be directly determined for each vehicle from Figure F-1 (for an annual mean wind speed of 12 km/hr). The effective drag coefficient, $C_{D_{eff}}$, is, as before, the product of F and C_{D_o}.

As can be seen, the wind-weighting factor, F, averaged about 1.08 (an 8% correction), ranging from 5 1/2% to almost 12%. Had this analysis been performed for a "B" cycle, the correction would be as high as 42%. (The wind vector is more of a factor at lower vehicle speeds; however, the aerodynamic component is smaller portion of the total energy requirements.)

---

[1] It should be noted that this is not a constant average speed, but rather a statistical average. For instance, an annual mean wind speed of 12 km/hr has winds of up to 50 km/hr occurring about 3% of the time and winds less than 12 km/hr occurring about 70% of the time.

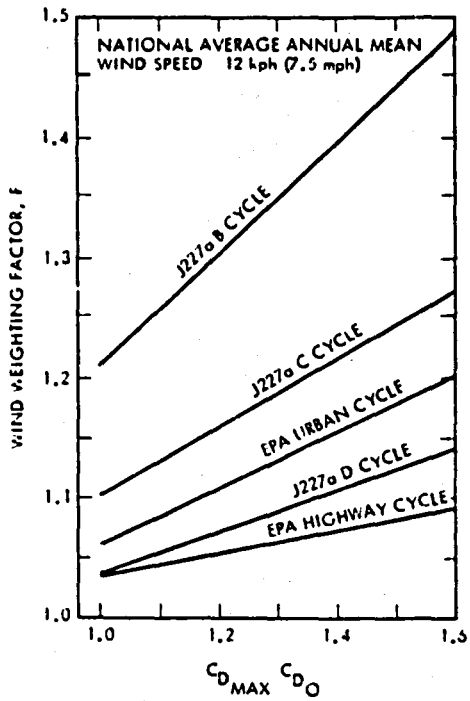

Figure F-1. Wind-Weighting Factors for Various Driving Cycles

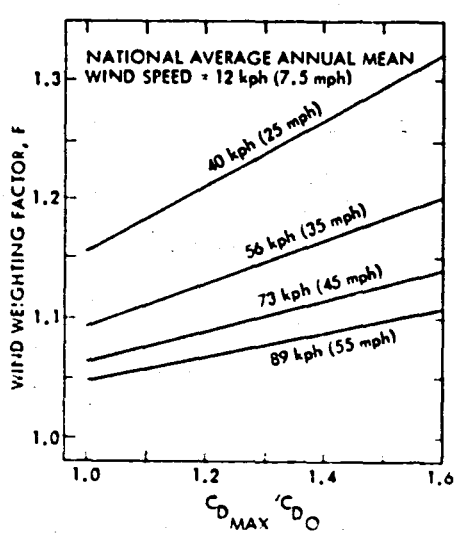

Figure F-2. Ambient Wind Drag Factor as a Function of Various Constant Speeds

Table F-3. Effective Wind-Weighted Drag of Test Vehicles Performing J227a D Cycles in the Presence of a 12 kph Annual Mean Wind Speed Equally Probable From Any Direction (Windows Closed)[1]

Vehicle	C_{D_o}	$C_{D_{max}}/C_{D_o}$	F	$C_{D_{eff}}$	$C_{D_{eff}}A$, m^2
GE ETV-1	0.308	1.27	1.084	0.333	0.614
Garrett ETV-2	0.395	1.50	1.124	0.444	0.9900
GE Centennial	0.337	1.12	1.058	0.357	0.660
CDA Town Car	0.367	1.16	1.065	0.391	0.686
SCT Rabbit	0.459	1.26	1.082	0.496	0.903
Sebring-Vanguard Citicar	0.541	1.20	1.072	0.580	0.986
Zagato Elcar	0.490	1.37	1.102	0.540	0.992
Jet 600 Van	0.530	1.40	1.107	0.586	1.138
Otis Van	0.581	1.30	1.090	0.633	1.641
Kaylor GT	0.583	(2)	-----	-----	-----
Energy R&D HEVAN	0.497	(2)	-----	-----	-----
AMC Pacer Wagon	0.406	1.27	1.085	0.441	0.980
AMC Pacer Sedan	0.450	1.24	1.079	0.486	1.079
Chevrolet Corvette	0.490	1.10	1.055	0.517	0.995
Oldsmobile Delta 88 Sedan	0.558	1.46	1.118	0.624	1.296
Chevrolet Chevette	0.502	1.14	1.062	0.533	0.941
Plymouth Horizon	0.411	1.32	1.093	0.449	0.880
Honda Civic Sedan	0.503	1.28	1.086	0.546	0.890
Honda Civic Wagon	0.514	1.22	1.076	0.553	0.932
Ford Fiesta	0.468	1.22	1.076	0.504	0.880

[1]With front windows open, the $C_{D_{max}}/C_{D_o}$ ratio increases by an average of 16% for this group of vehicle.

[2]Maximum C_D was not determined since test yaw angle was limited to 20 degrees.

END

DATE

FILMED

JAN 28 1981

End of Document